

Optical spectroscopy of Galactic field Classical Be stars

Gourav Banerjee,¹★ Blesson Mathew,¹ K. T. Paul,¹ Annapurni Subramaniam,² Suman Bhattacharyya¹ and R. Anusha¹

¹Department of Physics and Electronics, CHRIST (Deemed to be University), Hosur Main Road, Bangalore, India

²Indian Institute of Astrophysics, Koramangala, Bangalore, India

Accepted XXX. Received YYY; in original form ZZZ

ABSTRACT

In this study, we analyze the emission lines of different species present in 118 Galactic field classical Be stars in the wavelength range of 3800 - 9000 Å. We re-estimated the extinction parameter (A_V) for our sample stars using the newly available data from Gaia DR2 and suggest that it is important to consider A_V while measuring the Balmer decrement (i.e. D_{34} and D_{54}) values in classical Be stars. Subsequently, we estimated the Balmer decrement values for 105 program stars and found that $\approx 20\%$ of them show $D_{34} \geq 2.7$, implying that their circumstellar disc are generally optically thick in nature. One program star, HD 60855 shows $H\alpha$ in absorption- indicative of disc-less phase. From our analysis, we found that in classical Be stars, $H\alpha$ emission equivalent width values are mostly lower than 40 Å, which agrees with that present in literature. Moreover, we noticed that a threshold value of ~ 10 Å of $H\alpha$ emission equivalent width is necessary for FeII emission to become visible. We also observed that emission line equivalent widths of $H\alpha$, P14, FeII 5169 and OI 8446 Å for our program stars tend to be more intense in earlier spectral types, peaking mostly near B1-B2. Furthermore, we explored various formation regions of CaII emission lines around the circumstellar disc of classical Be stars. We suggest the possibility that CaII triplet emission can originate either in the circumbinary disc or from the cooler outer regions of the disc, which might not be isothermal in nature.

Key words: techniques: spectroscopic - stars: emission-line, Be - stars: circumstellar matter

1 INTRODUCTION

A classical Be (CBe) star is a special class of massive B-type main sequence star surrounded by a geometrically thin, equatorial, gaseous, decretion disc which orbits the star in Keplerian rotation (Meilland et al. 2007). The existence of such a circumstellar, gaseous disc was first suggested by Struve (1931). CBe stars belong to the luminosity classes III-V and their corresponding masses and radii range within $M_\star \sim 3.6 - 20 M_\odot$, and $R_\star \sim 2.7 - 15 R_\odot$ (Cox 2000). Rivinius et al. (2013) and Porter & Rivinius (2003) provide a review of studies carried out in the field of CBe star research till now. It is estimated that 10-20% of the B-type stars in our Galaxy are detected to be CBe stars from various studies such as Jaschek & Jaschek (1983); Zorec & Briot (1997); Mathew et al. (2008); Arcos et al. (2017).

Spectra of CBe stars show emission lines of different elements such as hydrogen, iron, oxygen, helium, calcium, etc. Spectral analysis of these lines provide a wealth of information about the geometry and kinematics of the gaseous disc and several properties of the central star itself. Hence, CBe stars provide an excellent op-

portunity to study circumstellar disc. Unlike protoplanetary dusty discs surrounding young stars, CBe star discs are not shrouded in dust. Moreover, the disc can be temporary, forming and dissipating on a timescale of years to decades which help us to study disc evolution. But, the disc formation mechanism of CBe stars - the ‘Be phenomenon’, is still not understood clearly. The physical model which best describes these discs so far is the viscous decretion disc (VDD) model (Carciofi et al. 2012; Lee et al. 1991).

Quite a number of spectroscopic surveys have been carried out until now to characterize CBe star disc and to better understand the ‘Be phenomenon’. Particularly important is the study of Jaschek et al. (1980) who classified CBe stars into five groups based on a sample of 140 stars observed over a period of 20 years. By studying a sample of 183 CBe stars over the entire sky, Slettebak (1982) found that the distribution is peaking at B2 spectral type. Later, Andrillat et al. (1988) performed the first systematic survey of CBe stars in the wavelength region 7500 - 8800 Å and drew attention to the fact that this region is poorly studied.

Subsequently, Mathew et al. (2008) studied 152 northern CBe stars in 42 open clusters through slitless spectroscopy. The spectral features of these stars were provided by Mathew & Subramaniam (2011). Paul et al. (2012) performed optical spectroscopy of 120

★ E-mail: gourav.banerjee@res.christuniversity.in (GB)

candidate CBe stars in the Magellanic clouds to study their spectral properties. Likewise, many other surveys have been performed both in the optical (e.g. [Andrillat & Fehrenbach \(1982\)](#); [Hanuschik \(1986\)](#); [Dachs et al. \(1986\)](#); [Banerjee et al. \(2000\)](#); [Koubský et al. \(2012\)](#); [Arcos et al. \(2017\)](#); [Klement et al. \(2019\)](#), etc.) and in the near-infrared ([Clark & Steele 2000](#); [Steele & Clark 2001](#); [Granada et al. 2011](#); [Mennickent et al. 2009](#)) regime to characterize CBe star discs. Spectroscopic studies of individual CBe stars have also been performed by different authors such as [Peton \(1972\)](#), [Koubský et al. \(2004\)](#), [Bhat et al. \(2016\)](#), [Smith et al. \(2017\)](#), [Paul et al. \(2017\)](#), [Mennickent et al. \(2018\)](#), [Levenhagen et al. \(2020\)](#), etc.

Our present work analyses the major emission lines present in a sample of 118 Galactic field CBe stars. These stars are well studied and have considerable amount of information available in literature. However, a comprehensive spectral analysis of all the emission lines present in the optical spectra of a sample of more than 100 field CBe stars is lacking in the literature. Our present study provides a collective understanding about the nature of emission lines seen in the spectra of 118 CBe stars, in the wavelength range of 3800 - 9000 Å. The analysis of the spectra incorporating the distance and extinction data provided by the Gaia DR2 catalog is helpful in understanding the properties of this large sample of CBe stars. Sect. 2 discusses the observations done and about the datasets used for this study. Analysis of various emission lines are discussed in Sect. 3. The prominent results from our study is summarised in Sect. 4.

2 OBSERVATIONS

2.1 Optical spectroscopy

The spectroscopic observations of the CBe stars were carried out with the HFOSC instrument mounted on the 2.1-m Himalayan Chandra Telescope (HCT) located at Hanle, Ladakh, India. During December 2007 to January 2009 we observed 118 CBe stars selected from the catalogue of [Jaschek & Egret \(1982\)](#). These stars were selected based on the observation visibility of HCT. The spectral coverage is from 3800 – 9000 Å. The spectrum in the ‘blue region’ is taken with Grism 7 (3800 – 5500 Å), which in combination with 167l slit provides an effective resolution of 10 Å at H β . The red region spectrum is taken with Grism 8 (5500 – 9000 Å) and 167l slit, providing an effective resolution of 7 Å at H α . Dome flats taken with halogen lamps were used for flat fielding the images. Bias subtraction, flat field correction and spectral extraction were performed with standard IRAF tasks. FeNe and FeAr lamp spectra were taken with the object spectra for wavelength calibration. All the extracted raw spectra were wavelength calibrated and continuum normalized with IRAF tasks. The log of our observations is presented in Table 1.

2.2 Gaia DR2 data

Gaia mission was launched by the European Space Agency (ESA) on December 19, 2013 as the successor to the Hipparcos mission. Its objective is to measure the distances, positions, space motions and perform photometry of over one billion stars in the Milky Way and beyond. The first data release - Gaia DR1, took place on September 14, 2016, followed by the second data release - Gaia DR2, on April 25, 2018. We used the newly available Gaia DR2 data to re-estimate the extinction parameter for our program stars. The analysis of spectral lines considering the Gaia DR2 data has added more meaning to our study.

3 RESULTS AND DISCUSSION

In this study, we analyze the emission lines of different species present in 118 Galactic field CBe stars. It is seen from the literature that 16 out of our 118 program stars are giants. Among these 16, 12 belong to luminosity class III, one star is of class II-III, another one of class III-IV, whereas two more are of class II (bright giants). We also found that 12 other stars are reported to be of class IV and another 4 stars belong to class IV-V. Similarly, one star among our sample, HD 45725 is reported to be a shell star. For our present study, we included all these candidates belonging to different luminosity classes.

Characterisation of our program stars according to their spectral types are done and is shown in Sect. 3.1. Sect. 3.2 reports the re-estimated distance and extinction values for our sample stars using the newly available data from Gaia DR2. Sect. 3.3 presents the study of all major spectral lines observed in emission in our stars. In the last section, results of Balmer decrement studies are reported and discussed. In that same section, we also carried out epoch-wise variation study of Balmer decrement for those stars having multiple measurements of Balmer decrement values in literature.

3.1 Spectral type distribution of the sample of CBe stars used in this study

In general, CBe stars belong within O9 to A3 spectral types. [Slettebak \(1982\)](#) found that the distribution of 183 stars of his sample peaked at B2 spectral type. By studying 94 CBe stars in 34 open clusters, [Mermilliod \(1982\)](#) reported the distribution to be peaking at spectral types B1–B2 and B7–B8. Subsequently, [Mathew et al. \(2008\)](#) also found the distribution in their sample peaks at B1–B2 and B6–B7 spectral types. Recently, [Arcos et al. \(2017\)](#) observed a similar distribution in $\sim 30\%$ of their sample 63 stars. The reason for this bimodal distribution observed in CBe stars is still not understood. [Mermilliod \(1982\)](#) suspected that only rapid rotation cannot account for such a distribution. Instead, he claimed that the observed distribution can be accounted for if special atmospheric conditions must be working in two restricted temperature ranges, influenced by radiation pressure and peaks in the opacity.

To characterize our program stars, we first checked the spectral type distribution in our sample. We were not able to receive better spectral type estimates from our data since our spectral resolution is lower than various previous studies performed by other authors. Hence, we adopted the spectral type for every star from the literature (shown in Table 1). We found that the distribution of our program stars is also peaking at B1-B2 and again at B7-B8 spectral types, in good agreement with previous studies. Fig. 1 shows the histogram of CBe star incidence in our sample. Among our 118 stars, 26 ($\sim 22\%$) belong to B2 and 12 stars belong to B8 spectral types. Observing such a similar trend in both field and cluster CBe stars by various authors is interesting and might be real. Hence, we suggest further investigation to be carried out to look into this trend of bimodal distribution observed in CBe star spectral types.

3.2 Re-estimation of the extinction parameter using Gaia DR2

Before getting into spectral line studies, we characterized our sample stars using the newly available data from Gaia DR2. We found that 83 of our 118 stars have parallax values in Gaia DR2. The distance (in parsec) for these 83 stars are adopted from [Bailer-Jones et al. \(2018\)](#). The obtained distance for these 83 stars is presented in

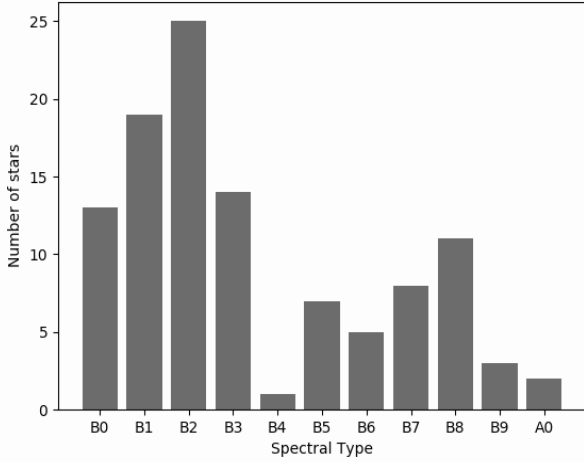


Figure 1. Histogram showing the incidence of CBe stars in our sample. It is clearly visible that the distribution of our program stars is also peaking at B1-B2 and again at B7-B8 spectral types, in good agreement with previous studies.

Table 2. Column 2 of Table 2 lists the determined distance for each case with an upper and lower limit of error. It is seen from the Table that the distance ranges between 130 – 3430 pc. According to our estimate, HD 53367 (130 pc) is the closest star in our sample, whereas MWC 566 (3430 pc) is the farthest. HD 21455 has the minimum error in distance, 169^{+1}_{-2} pc.

Following this, we re-estimated the extinction parameter, i.e. A_V for those stars using the adopted distance. This is done using the distance modulus relation. The observed apparent magnitude (m_V) is listed in Table 1. Absolute magnitude (M_V) is adopted from Pecaut & Mamajek (2013) using the object’s spectral type obtained from literature. Using these m , M and distance values in the distance modulus relation, the extinction A_V is calculated for 83 stars. The A_V obtained by this method is the sum of the interstellar extinction and the circumstellar emission from the respective CBe star disc.

The re-estimated extinction (A_V) for 83 stars is presented in Column 3 of Table 2. For the rest 35 cases, we adopted the respective A_V value from the literature. Table 3 presents the A_V value for those 35 cases. We found that A_V value for our stars mostly (in 48 cases, $\approx 58\%$) range between 0 - 0.4. For another 13 out of 83 stars, A_V ranges between 0.4 - 1.0, whereas $A_V \geq 1.0$ in the rest 22 cases.

Next, we used interstellar dust maps to check the contribution of the interstellar extinction component for our sample stars. The dust extinction maps of Green et al. (2019) are used to estimate the interstellar extinction component of our CBe stars. We found that in most cases, A_V determined through this method matches with our photometric estimate. This suggests that there is no appreciable contribution to A_V from the circumstellar disc, i.e. contribution of the circumstellar emission component is much less. However, for $\sim 40\%$ cases, the A_V value estimated through photometry is higher (0.2 - 0.4 mag) than those obtained from the dust map. This implies that the circumstellar component is more prominent in those cases than the corresponding interstellar component.

Hence, we suggest that A_V is of much importance and has to be taken into account for the analysis of CBe star properties. A_V values estimated in this study is used for extinction correction in the analysis of Balmer decrement in CBe stars (discussed in Sect. 3.4).

3.3 Spectral line analysis for the program stars

This section describes all major emission lines observed in our 115 field CBe stars covering the whole wavelength range of 3800 – 9000 Å. According to the best of our knowledge, this is the first study where near simultaneous spectra covering the whole spectral range of 3800 – 9000 Å has been studied for over 100 field CBe stars. Fig. 2 shows a representative sample spectra of one of our program star HD 55606. The average signal-to-noise ratio (SNR) of the spectra of every CBe star used for this study is greater than 100.

3.3.1 Balmer series of Hydrogen lines

All the CBe stars used in the present study are identified based on their $H\alpha$ emission, as catalogued in Jaschek & Egret (1982). In a CBe star, recombination emission lines such as $H\alpha$ are formed in the circumstellar disc. The shape of the emission profiles are explained as a dependency of the inclination angle (i) of the star’s rotation axis to observer’s line of sight (Hanuschik et al. 1996). For example, single-peak and wine bottle profile suggests that the star is viewed pole-on ($i = 0^\circ$), shell profiles when the disc is viewed along the equator ($i = 90^\circ$) and double-peaked profiles at mid-inclination angles (Porter & Rivinius 2003; Catanzaro 2013).

Majority of our sample ($\approx 60\%$; 68 stars) has $H\alpha$ in normal, single-peaked emission. Although due to our low resolution, a few cases where the profile appears as a single peak can be double-peak if the resolution is higher. The $H\alpha$ profile is in double-peaked emission (*dpe*) in 5 stars, core emission (*ce*) in 12 stars and absorption in emission (*ae*) in 3 cases. Another 10 stars show emission in absorption (*eia*) profile, whereas the rest 20 stars are weak emitters with $H\alpha$ EW < -5.0 Å. Since CBe stars with single-peaked $H\alpha$ emission is quite common among our sample, we have not discussed each of them in detail. The equivalent width (EW) of $H\alpha$ emission line in our observed stars range within -0.5 to -72.7 Å, where the negative sign suggests that $H\alpha$ is in emission. An error of $\pm 10\%$ exists in the measurement of the EW. The star MWC 566 possesses the highest value of $H\alpha$ EW of -72.7 Å, whereas HD 61205 shows the minimum $H\alpha$ EW of -0.5 Å.

Since in-filling of photospheric absorption lines occur, visual inspection is not reliable in discerning between a star showing weak emission and another one exhibiting no emission at all. Hence, we calculated the $H\alpha$ EW for all our stars first and then measured the absorption component at $H\alpha$ line from the synthetic spectra using models of stellar atmospheres (Kurucz 1993) for each spectral type. The photospheric contribution from the underlying star is added to the emission component to estimate the corrected $H\alpha$ EW. Through this process, we were able to identify 20 stars which are weak emitters, showing $H\alpha$ EW < -5.0 Å.

We looked into the literature to check the range of $H\alpha$ EW reported by some other studies such as Barnsley & Steele (2013), Mathew & Subramaniam (2011), Slettebak et al. (1992), Hanuschik (1988) and Dachs et al. (1986, 1992). These works were particularly selected to collect CBe star samples from a variety of locations (such as northern and southern hemisphere) and environments (like fields and clusters) in our galaxy. While Barnsley & Steele (2013), Slettebak et al. (1992) and Hanuschik (1988) observed 55, 41 and 26 northern CBe stars respectively, Dachs et al. (1986, 1992) studied a sample of 55 and 37 southern CBe stars. On the other hand, Mathew & Subramaniam (2011) presented the results of a survey of 152 cluster CBe stars.

Fig. 3 shows the distribution of $H\alpha$ EW for CBe stars observed by these authors compared to that seen for our program stars (cor-

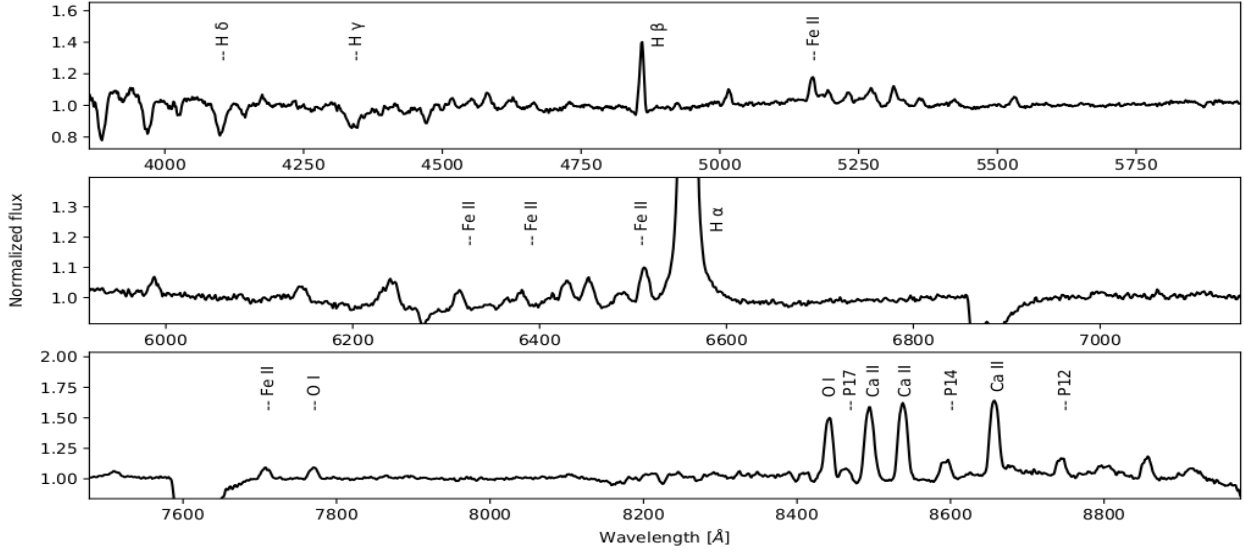


Figure 2. Representative spectra of our sample star HD 55606 showing different spectral features in the wavelength range of 3800 - 9000 Å.

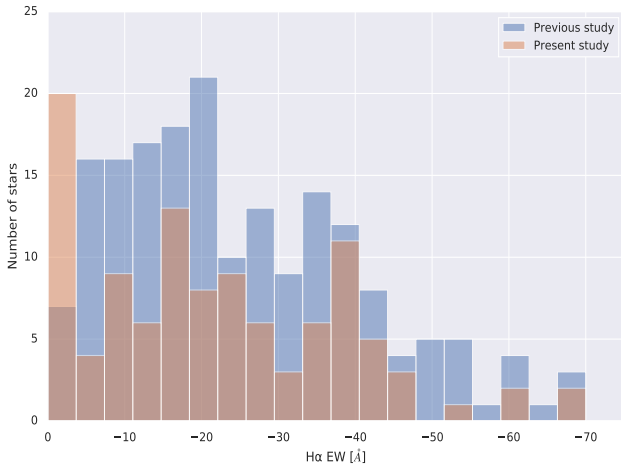


Figure 3. $H\alpha$ equivalent width distribution of CBe stars in our sample compared with selected previous studies such as Barnsley & Steele (2013), Mathew & Subramaniam (2011), Slettebak et al. (1992), Hanuschik (1988) and Dachs et al. (1986, 1992).

rected for the underlying stellar absorption). It is clearly visible from Fig. 3 that for our sample, $H\alpha$ EW mostly are lower than -40 Å with a peak somewhere near -20 Å. The binning scheme we employed here is the rule of square roots. Looking into previous surveys, we find that the $H\alpha$ EW mostly range within -5 to -40 Å peaking near -20 Å. Moreover, we observe in our study that a second peak appears somewhere between -35 and -40 Å. It is important to mention that the $H\alpha$ EW is a variable parameter and hence some difference seen in Fig. 3 can be due to this aspect.

CBe stars are known to show variability in spectral line profiles. The extreme case of such a variability is the disappearance of $H\alpha$ emission line, indicative of disc-less state in CBe stars. The spectrum will then look like that of a B-type star with photospheric

absorption lines. A well studied example is the disc-less episode of X Persei (Norton et al. 1991). Observations during such a disc-less state can be used to estimate the stellar parameters such as spectral type and luminosity since the spectral lines are unaffected by veiling from the disc (Fabregat et al. 1992). During our observation campaign we also identified one star (HD 60855) showing $H\alpha$ in absorption. The measured and corrected $H\alpha$ EW for our sample stars are shown in Table 4, where HD 60855 is marked in bold. However, in order to understand whether it is going through disc-less episode, we need to check through stellar atmospheric profiles, which is an ongoing study. A representative sample of the $H\alpha$ line profiles for our program stars is shown in Fig. 4.

Among 115 stars, 110 show $H\beta$ line either in emission or emission in absorption. $H\beta$ is present in absorption in 3 other cases after correcting for the underlying stellar absorption. Grism 7 spectra is not available for the stars HD 45726 and HD 58343, thus we could not observe the $H\beta$ line for them. $H\beta$ emission line EW of our stars range between -0.3 to -12.8 Å. HD 23552 shows the highest value of $H\beta$ EW of -12.8 Å, while HD 20134 exhibits the minimum $H\beta$ EW of -0.3 Å. Two stars, namely HD 45910 and HD 50820 show P-Cygni nature of $H\beta$ emission profile.

When it comes to $H\gamma$ line, 98 stars show it in emission. $H\gamma$ emission line EW for our program stars range between -0.3 to -10.8 Å. Both HD 23552 and HD 237060 possess the highest value of $H\gamma$ EW of -10.8 Å, whereas HD 37967, HD 47359 and MWC 500 show the minimum $H\gamma$ EW of -0.3 Å.

3.3.2 Paschen series of Hydrogen lines

Unlike Balmer lines, emission lines of the Paschen series is a less studied area in CBe star research. In the region $7500 - 10000$ Å, higher order lines of the Paschen series are visible starting from P9 or P10 right up to P23. Among these, P14 is the line which can provide the most accurate EW measurement since it is not blended with any other feature. Only a few scattered studies exist addressing the occurrence of prominent Paschen lines in CBe stars.

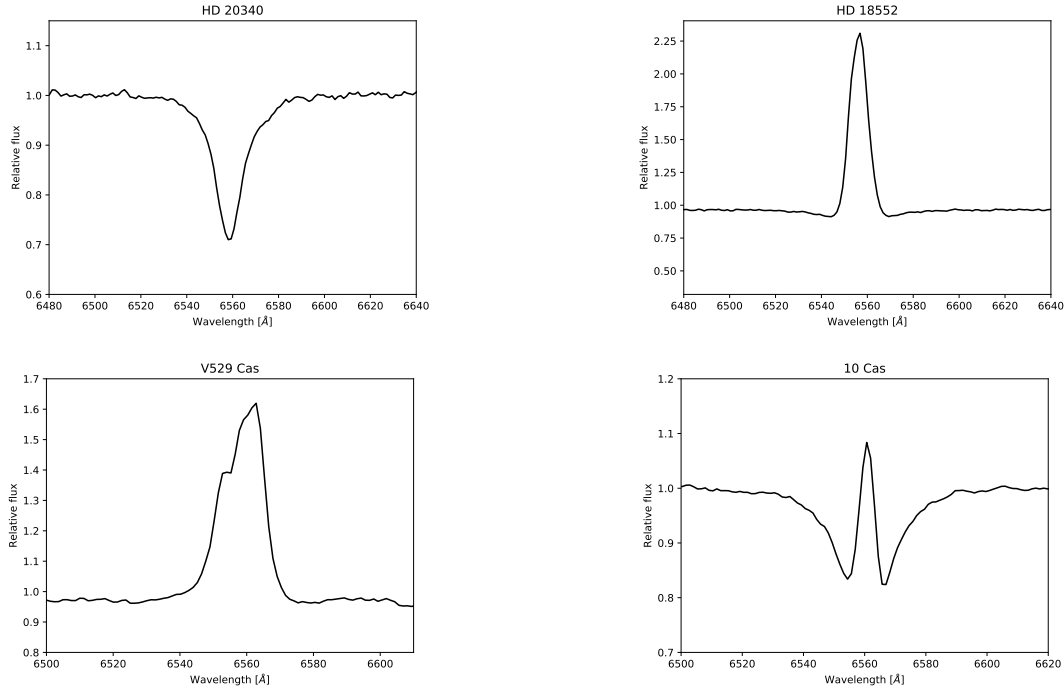


Figure 4. H α line profiles for our sample stars HD 20340, HD 18552, V529 Cas and 10 Cas. It is noticed that HD 20340 apparently shows H α in absorption, whereas the other 3 stars HD 18552, V529 Cas and 10 Cas show H α line in normal emission, double-peak emission and emission in absorption, respectively.

Andrillat & Houziaux (1967) studied Paschen lines in CBe stars for the first time and identified Paschen lines from P9 – P26 in their sample. Mathew et al. (2012b) discussed Paschen lines while studying the OI 8446 Å line in 26 CBe stars. Among our sample, 47 ($\approx 40\%$) stars show Paschen lines in emission, whereas in 54 cases they are present in absorption. Out of those 47, 39 stars belong to spectral types earlier than B5. This is in agreement with Briot (1981), who noticed that Paschen emission lines are mostly observed in CBe stars of earlier type. Additionally, we noticed that in 36 out of these 47 stars, only Paschen lines are visible in emission, whereas in 11 cases both Paschen and CaII triplet lines are present in emission.

Briot (1981) noticed that the emission strength of Paschen lines gradually decreased from P12 to the series limit in all CBe stars, irrespective of the spectral type. Unlike to that of Briot (1981), we also observed a trend in Paschen emission lines from a larger sample of CBe stars. In our study, this trend in the emission strength distribution is used for deblending the Paschen emission components from CaII triplet emission lines.

3.3.3 CaII triplet emission lines

CaII triplet (8498 Å, 8542 Å, 8662 Å) emission lines are low ionization lines which are formed in a region having temperature $T \sim 5000$ K (Polidan & Peters 1976). It was Hiltner (1947) who first identified CaII triplet emission in the spectra of CBe stars. CBe star discs are known to be hot in nature, with disc temperature ranging within 10,000 – 20,000 K (Mathew et al. 2012a; Sigut & Jones 2007). Hence, CaII lines are not expected to be seen in emission for CBe stars. But, interestingly, CaII triplet emission lines are observed occasionally in the spectra of CBe stars, which become quite prominent in some cases.

The fraction of CBe stars showing CaII triplet emission remains

unclear till now. Polidan & Peters (1976) and Shokry et al. (2018) found CaII triplet in $\approx 20\%$ of their surveyed stars. Andrillat et al. (1988) observed CaII triplet in 11 out of their 40 sample stars ($\approx 27\%$). On the contrary, Mathew & Subramaniam (2011) noticed CaII triplet emission in $\approx 60\%$ of their sample of 152 cluster CBe stars. Surprisingly, although Shokry et al. (2018) observed CaII triplet in absorption in few of their program stars, they are not expected to be visible in absorption in CBe stars as these stars are too hot for forming CaII absorption lines.

Through our present study we evaluated the percentage of CBe stars showing CaII triplet emission in our sample. In order to do that, we needed to deblend the Paschen line contribution from the emission lines in CaII triplet wavelength region. This process of deblending is explained below.

3.3.3.1 Subtracting the CaII emission components from the corresponding Paschen components

We found that only 17 of our 115 stars show CaII lines in emission. This corresponds to $\approx 15\%$, which is in agreement with earlier results obtained by Polidan & Peters (1976); Andrillat et al. (1988); Shokry et al. (2018). Interestingly, Briot (1981) did not observe CaII triplet in the star γ Cas. But we found CaII emission to be present for this star in our study, similar to what was observed by Koubský et al. (2012).

In low resolution spectra, similar to ours, CaII 8498, 8542, 8662 Å lines often get blended with the Paschen lines P16 (8502 Å), P15 (8545 Å) and P13 (8665 Å), respectively. So, to identify CaII lines, it is necessary to remove the Paschen emission from the net emission strength associated with the wavelength region of CaII triplet. It may be noted that in cases where CaII triplet is present, the emission lines at 8498, 8542 and 8662 Å appear to be more intense than the adjacent Paschen lines.

In order to take out the CaII component, we first looked at those 36 of our program stars showing only Paschen emission lines. We noticed that P14 is the most intense line among P12 – P19 which is not affected by any other feature. Out of these 36 stars, 34 exhibit P14 in emission. We measured the EW for P14 and the adjacent lines such as P12 – P17 for all these cases. It is observed that the P14 EW is matching within $\sim 15\%$ with respect to other lines. For example, for the star HD 21212, P12 EW is -4.4 \AA , whereas P14 and P17 EW are -4.2 and -4.5 \AA , respectively. Then, we looked into those 11 cases where CaII triplet emission is blended with Paschen lines. Now for each star, we subtracted the P14 EW from the blended CaII lines. This exercise is performed to take out the Paschen component out of the composite line.

Subsequently, we estimated the emission strength ratio of CaII 8498:8542:8662 \AA lines is 1:1:1 for nine cases which is quite different from the theoretically predicted value of 1:9:5 (Osterbrock & Ferland 2006; Polidan & Peters 1976). The theoretically predicted emission strength ratio 1:9:5 corresponds to an optically thin scenario whereas a deviation from this considers the line forming region as optically thick. For two other cases (HD 38010 and V782 Cas) this ratio corresponds to around 1:2:1 and for γ Cas it is 1:4:3.

3.3.3.2 CaII triplet line formation region: possibility of binarity

In case of young stellar objects it is suspected that CaII triplet emission occurs commonly due to the processes of accretion and magnetism (Moto’oka & Itoh 2013; Kwan & Fischer 2011), or a combination of both. For cataclysmic variables, Ivanova et al. (2004) suggested that CaII formation is more confidently linked to external UV irradiation of an optically thin gas. Since large scale magnetic fields have not been observed in CBe stars, the UV photons originating from accretion shocks become the most promising mechanism that can power the CaII triplet formation. But, since CaII emission is not detected in all CBe stars, Shokry et al. (2018) claimed that the self re-accretion process in CBe stars from the viscous disc may be insufficient. Through this line of argument they arrived at the conclusion that binarity is the only possible explanation.

We analyzed CaII triplet lines in our sample by a different approach of deblending the CaII components from their Paschen counterparts and detected the relative intensity ratios of the triplet lines. Our analysis implies that the gas which gives rise to CaII emission is optically thick in nature. But as it is mentioned earlier, CaII emission lines can be produced only in a dense, cool region ($T \sim 5000\text{K}$ or so) around CBe stars. Hence, our study indicates two possible regions where CaII lines can form:

1. The CaII triplet emission line forming region might be in the circumbinary disc of the CBe stars.

2. The CBe star disc may not be isothermal in nature, due to which the outer regions can be cooler, where CaII emission can originate.

To check the binary hypothesis, we searched in literature whether any of our 17 stars showing CaII emission are binaries or not. We found that 5 out of 17 are binary stars. Three among them, namely HD 25940 (Wang et al. 2018), HD 55606 (Chojnowski et al. 2018) and HR 2142 (Schootemeijer et al. 2018) have been reported to be binary systems containing a CBe star primary and a sdO (sub dwarf O type) companion. HD 45910 is a known interacting binary

system (Koubský et al. 2012, 2011), whereas γ Cas is also suggested to be a binary system having a possible compact object as a companion (Smith et al. 2017). On the contrary, Borre et al. (2020) suggested that the X-ray emission in case of γ Cas might be coming from the CBe star itself, thus ruling out the binarity scenario.

It is to be noted that the nature of the binary companion must also be considered to test the binary hypothesis for CaII emission formation in CBe star discs. Sub dwarf OB (sdOB) stars possess masses of $\sim 1 M_{\odot}$ and temperatures up to 50000 K (Klement et al. 2019). Being hotter than the CBe stars, Klement et al. (2019) suggested that the radiation from their sdOB companions can heat up the outer disc region of the primary CBe star. Hence, it is difficult to create a cool, dense region from where CaII emission can originate. This argument holds good for γ Cas also where the binary companion is suggested to be a compact object (Smith et al. 2017). Moreover, HD 45910 in our sample shows CaII emission, whereas HD 218393 does not show any CaII emission, though it is also known to be an interacting binary system (Koubský et al. 2011). Furthermore, Koubský et al. (2012) pointed out that various other binaries (RX Cas, CX Dra, β Lyr) in their sample also do not exhibit any CaII emission. Therefore, the possibility of binary origin for CaII emission lines is not supported by the above studies.

Next, we look into the non-isothermal disc scenario. Assuming CBe star discs to consist only of hydrogen, the disc temperature structure is expected to be mostly isothermal with an exception of a temperature dip that appears in the vicinity of the central star (Carciofi & Bjorkman 2006, 2008). However, models assuming more realistic chemical mixing processes indicate that the temperature structure may be more complex (Jones et al. 2004; McGill et al. 2013). Hence, the non-isothermal disc scenario appears to be a promising one.

But, since CaII line analysis has been possible for only 17 of our program stars, it is too early to provide a conclusion regarding the formation region of CaII emission lines. We would further like to address this issue by looking into larger samples of CBe stars including various environments such as clusters and regions of different metallicity. Nevertheless, the binarity hypothesis also cannot be ruled out completely as of now.

3.3.4 FeII emission lines

Apart from hydrogen and calcium, FeII emission lines are commonly visible in the spectra of CBe stars (Slettebak et al. 1992). Various FeII lines (belonging to different multiplet series) have been detected in CBe stars, 5169 \AA (multiplet no. 42) being apparently the strongest optical FeII line (Hanuschik 1987). Other commonly observed FeII emission lines in CBe stars are 4584 \AA (multiplet 38), 5317 \AA (49), $5198, 5235, 5276 \text{ \AA}$ (49), 5284 \AA (41), 5363 \AA (48), 6516 \AA (40) and 7712 \AA (73) (Apparao & Tarafdar 1994a; Mathew & Subramaniam 2011).

It is seen that studies based on FeII emission lines in CBe stars are less in literature when compared to H α lines. This less attention may be due to the fact that Fe emission lines are rather difficult to detect. However, the first detailed high-resolution study for FeII emission lines observed in CBe stars was performed by Hanuschik (1987). A few later studies were performed to understand the FeII emission forming region in CBe stars (e.g. Hanuschik (1988); Jaschek et al. (1993); Arias et al. (2006)). There exist a few other studies which concentrated on better understanding the geometry and kinematics of CBe star envelopes using FeII emission lines (e.g. Slettebak et al. (1992); Dachs et al. (1992); Hanuschik

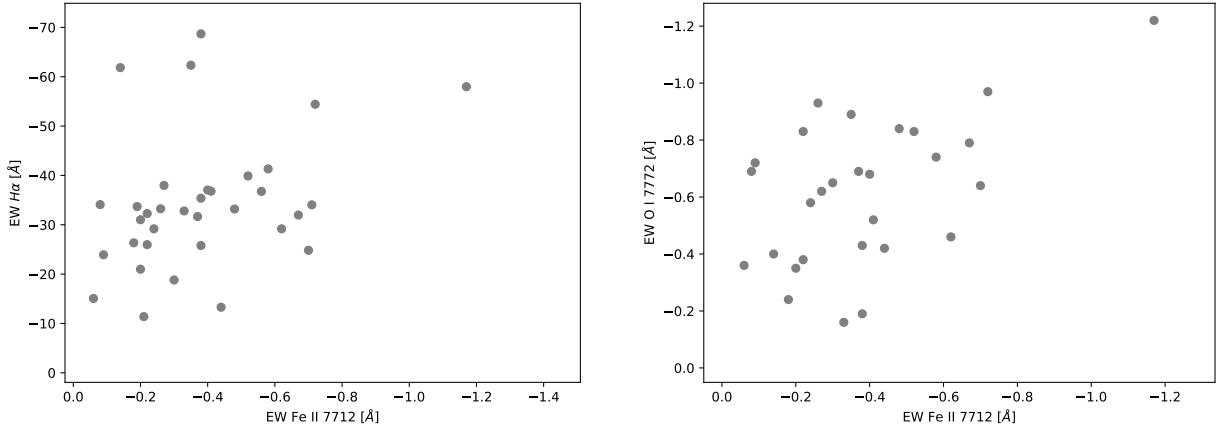


Figure 5. Measured EW of H α and O I 7772 Å emission lines plotted against the Fe II 7712 Å emission line for our program stars. Though no substantial correlation is found in both cases, it is clearly visible that a minimum H α EW (~ -10 Å) is necessary for Fe II 7712 Å emission to become visible.

(1994); Tarafdar & Apparao (1994); Ballereau et al. (1995); Jones et al. (2004); Arias et al. (2006)).

We found that 95 ($\approx 83\%$) stars in our sample show Fe II emission lines in their spectra, in agreement with Mathew & Subramaniam (2011). In total, 43 different Fe II emission lines are identified belonging to different multiplets. Among them, 5169 Å is the most common, present in emission in 37 cases. Other prominent emission lines observed are 5317 Å (36 cases) followed by 5018 Å (multiplet 42) present in 24 cases, 5235 Å (21 stars), 5276 Å (21 cases), 6516 Å (20 stars), 5363 Å (19 cases), 5198 Å (17 cases) and 4584 Å (10 cases).

We noticed that comparatively less studies have been performed for Fe II emission lines that belong to the region beyond 7500 Å, especially for the 7712 Å line. Among our sample, 34 out of 115 stars ($\approx 30\%$) exhibit Fe II 7712 Å line in emission. Out of these, 32 have spectral types earlier than B6, in agreement with Ballereau et al. (1995) and Andrillat et al. (1988).

3.3.4.1 Correlation between Fe II 7712 Å and H α line

Hanuschik (1987) and Slettebak et al. (1992) observed that in CBe stars, the EW of the emission strength of H α line correlates with that of Fe II lines. To verify this, we looked into the EW of the emission component of H α line for all 34 of our program stars as a function of Fe II 7712 Å emission. The result is shown in Fig. 5.

From Fig. 5, it is noticed that H α EW is not correlated with that of Fe II 7712 Å line. But it is clearly visible that a minimum H α EW is indeed necessary for Fe II 7712 Å emission to become visible. We found this minimum H α EW for our sample to be over ~ -10 Å, though 30 out of our 34 stars which show Fe II 7712 Å emission have H α EW of over -20 Å. Among these 34 stars, HD 58343 shows the minimum EW due to which we fixed the lower limit for H α EW to be ~ -10 Å. Studying a sample of 17 bright southern CBe stars, Hanuschik (1987) also suspected that a minimum EW for H α (over -7 Å) is essential for Fe II lines to become visible. Hence, our study strongly supports the results of Hanuschik (1987).

3.3.4.2 Correlation between Fe II 7712 Å and Paschen emission lines

In our sample, 28 out of these 34 stars which show Fe II

7712 Å in emission also exhibit Paschen emission lines. Three others show Paschen lines in absorption (AS 52, HD 25940 and HD 37115), whereas for the remaining three (HD 12302, HD 45910 and HD 237118) no Paschen lines are visible. This result is in fair agreement with Andrillat et al. (1988) who noticed that whenever Fe II is in emission (in 12 of their program stars), Paschen lines are also found in emission, except one (HD 192044 – a B7 star) case where Paschen lines were in absorption. One of our program stars, namely HD 37115, which shows Fe II in emission and Paschen in absorption is also of B7 type.

3.3.4.3 Correlation between Fe II 7712 Å and O I 7772 Å line

We noticed that 28 out of our 34 stars which show Fe II 7712 Å line also exhibit O I 7772 Å line in emission. This result does not agree with Andrillat et al. (1988) who noticed that whenever Fe II 7712 Å is in emission, O I 7772 Å is also observed in emission. Hence, similar to Andrillat et al. (1988) we can conclude that in general, both Fe II 7712 Å and O I 7772 Å are either together visible in emission, but not in every individual case.

We then investigated our sample 29 stars showing both Fe II 7712 Å and O I 7772 Å emission lines to search for any possible correlation between the measured EW of these two lines. Fig. 5 shows our result. The correlation coefficient is found to be 0.29 which implies that no correlation is present between these two lines.

3.3.5 O I emission lines

Like Balmer, Paschen and Fe II lines, O I 8446 Å is another common line observed in CBe stars, mostly in emission and rarely in absorption. This line is comparatively more studied than its counterpart O I 7772-4-5 Å triplet, another O I line feature often found in CBe stars. O I 8446 Å line gets blended with the P18 line, whenever both are seen in emission (Mathew et al. 2012b). Kitchin & Meadows (1970) observed a strong correlation between the H α and O I 8446 Å EW which was subsequently supported by the study of Andrillat et al. (1988).

It is noticed that the O I 8446 Å is around 4 times stronger than the O I 7772 Å line. Bowen (1947) first proposed that Lyman- β (Ly β) fluorescence process may be the possible O I 8446 Å line excitation mechanism in CBe stars. Later, Mathew et al. (2012b) indeed identified Ly β fluorescence to be the primary O I 8446 Å line

excitation mechanism in CBe stars. Mathew et al. (2012b) also concluded that Or emission originates from relatively inner regions (mean size of 0.71 ± 0.27 of the $H\alpha$ emission region size) of the envelope, i.e. regions having higher density.

Or 8446 Å line is present in emission in 66 ($\approx 57\%$) of our program stars. Among them, 42 stars show both Or 8446 Å and Or 7772 Å lines in emission. Paschen lines are absent in 24 out of these 66 stars. Since the Or 8446 Å line gets blended with the P18 line of the Paschen series, measuring the EW of the Or 8446 Å line becomes difficult if Paschen lines are present. Among the 24 stars where Paschen lines are not present, HD 12302 has the highest value of Or 8446 Å EW (-3.9 Å).

Or 7772 Å line, the counterpart of Or 8446 Å, is also observed in CBe stars. Jaschek et al. (1993) determined the outer radius of the envelope producing Or 7772 Å line to be 1.78 ± 0.82 stellar radii. Collisional excitation is regarded as the contributor for this Or 7772 Å line formation instead of $Ly\beta$ fluorescence. Andrillat et al. (1988) found that Or 7772 Å is seen in emission mostly in CBe stars having spectral types earlier than B2.5, whereas stars later than B2.5 show it mostly in absorption. Later, Jaschek et al. (1993) found that Or 7772 Å is always present in emission in CBe stars.

In our sample, Or 7772 Å line is seen in emission in 44 ($\approx 38\%$) stars, while 34 stars show it in absorption. This result does not agree with Jaschek et al. (1993) who observed that Or 7772 Å is always present in emission in CBe stars. Most of the stars showing Or 7772 Å in absorption have very weak absorption lines, suggesting the presence of some amount of emission in this line. But a few stars actually show sharp absorption line of Or 7772 Å, thus not agreeing with the results of Jaschek et al. (1993). Noticeable absorption lines of Or 7772 Å observed in stars such as HD 15238, HD 37806, HD 45626 and HD 51480 raise the possibility of self-absorption process being active in CBe star envelopes. We found that 35 among these 44 stars showing Or 7772 Å emission are earlier than B3 spectral type, which is in agreement with Andrillat et al. (1988).

We then carried out the correlation study between the Or 7772 Å and Paschen lines. We found that 40 out of our observed 44 stars which show Or 7772 Å line in emission also show Paschen lines in emission. This result does not agree with Andrillat et al. (1988) who noticed that in CBe stars whenever Or 7772 Å line is in emission, Paschen lines are also visible in emission. Hence, we could not confirm the correlation between the presence of Or 7772 Å and Paschen lines as observed by Andrillat et al. (1988). Further investigations with larger sample of stars is suggested to establish any such correlation.

3.3.6 HeI emission lines

HeI lines are generally formed in high temperature regions with $T \sim 15,000$ K. In CBe stars, HeI lines are usually not expected to be seen in emission since their disc temperature is less. Instead, these lines are present in absorption in the spectra of early-type CBe stars, i.e. B0 - B5. Emission lines of HeI are usually visible in regions containing high ionization plasma such as symbiotic stars (Siviero & Munari 2003). However, we find HeI lines in emission in CBe stars in rare cases. Study of HeI emission lines is another less explored area in CBe star research.

Bahng & Hendry (1975) found HeI lines 5876 and 6678 Å in emission in the spectra of the star κ CMa (B1.5 IVe) while lines in the blue region such as 4026 and 4471 Å were observed in absorption. They claimed HeI emission lines to be originating in the circumstellar envelope around 2 stellar radii from the central star. They also suggested that these lines may either be a temporary

phenomenon or non-LTE effects are responsible for their selective excitation. Chalabaev & Maillard (1985) observed HeI lines for few CBe stars, such as the 10830 Å line for γ Cas. Lennon & Dufton (1989) proposed the inclusion of UV line blanketing in the theoretical models as a solution to the problem. Subsequently, Dachs et al. (1992) identified HeI 5876 Å line in emission in 7 out of their sample of 37 southern CBe stars.

Later, Apparao & Tarafdar (1994b) claimed that in CBe stars, HeI emission lines can be produced by some compact binary companion which is accreting matter from the primary (here the CBe star) star's disc. On the contrary, analysis of HeI lines for the star λ Eri (B2IVne) by Smith et al. (1997) suggested that these lines are formed in some critical density region where collisional and radiative de-excitations are comparable. They predicted Lyman pumping mechanism to be responsible for HeI line emission in B0 – B5 stars.

In our sample, we found HeI 5876, 6678 and 7065 Å lines in emission in 13 ($\approx 11\%$) stars. We noticed that 12 out of these 13 stars belong to spectral types B3 or earlier, 6 among them being B0 type. Single-peaked emission is observed in 6 out of 13 stars (γ Cas, HD 23552, HD 244894, CD-22 4761, MWC 3 and MWC 5). Interestingly, each star shows some notable characteristic in HeI emission.

While all three HeI lines in the red region, 5876, 6678 and 7065 Å are visible in HD 23552, CD-22 4761, MWC 3 and MWC 5; γ Cas and HD 244894 show only 5876 and 7065 Å lines in emission. The 7065 Å line is very intense in MWC 3 than others. Double-peaked emission is seen in case of HeI 5876, 6678, 7065 Å lines in HD 13051 and one star (HD 49330) shows P-Cygni profiles for HeI 5876, 6678 Å lines. For the rest 5 among 13 stars, HeI lines exhibit shell features. All three 5876, 6678, 7065 Å lines are observed to be in shell profiles in HD 12856, HD 50696 and MWC 667, whereas shell profile signatures in HeI 5876 and 7065 Å are visible in V746 Mon. On the other hand, HeI 5876, 6678 Å show shell features in MWC 149, whereas 7065 Å line is present in normal emission profile.

However, we did not find any HeI emission line in the blue region (such as 4026, 4142, 4387, 4471 Å) in any of our program star except for CD-22 4761 where 4142, 4387, 4471 Å lines show filled-in profiles. Fig. 6 displays the HeI emission line profiles for two of our program stars.

Our result, thus indicates that hotter CBe stars of earlier spectral types might have high disc temperature, thus showing HeI in emission. The only exception is HD 23552 which shows HeI emission lines, though it is of B8 type. This is an interesting case which needs further scrutiny.

3.3.7 Spectral type dependency of our program stars with respect to Equivalent Width

We found that the emission line EW for our program stars tend to be more intense in earlier spectral types. Fig. 7 shows the distribution of $H\alpha$, P14 (8598 Å), FeII 5169 Å and Or 8446 Å line EW with respect to spectral types for our stars. Here, we observe that $H\alpha$ EW attain a maximum value somewhere near B1-B2 spectral types and gradually decrease towards late-types. P14 and Or 8446 Å line also show a somewhat similar trend where we find that EW becomes highest for early type CBe stars around B2. Emission strength of Or 8446 Å decreases for later types similar to $H\alpha$ emission.

Hence, it seems that the emission strength of $H\alpha$, P14 and Or 8446 Å is more in early B-type stars. FeII 5169 Å EW also shows a trend of peaking near B1-B2 even if we remove the single data point lying near the -1.2 Å region in the respective plot.

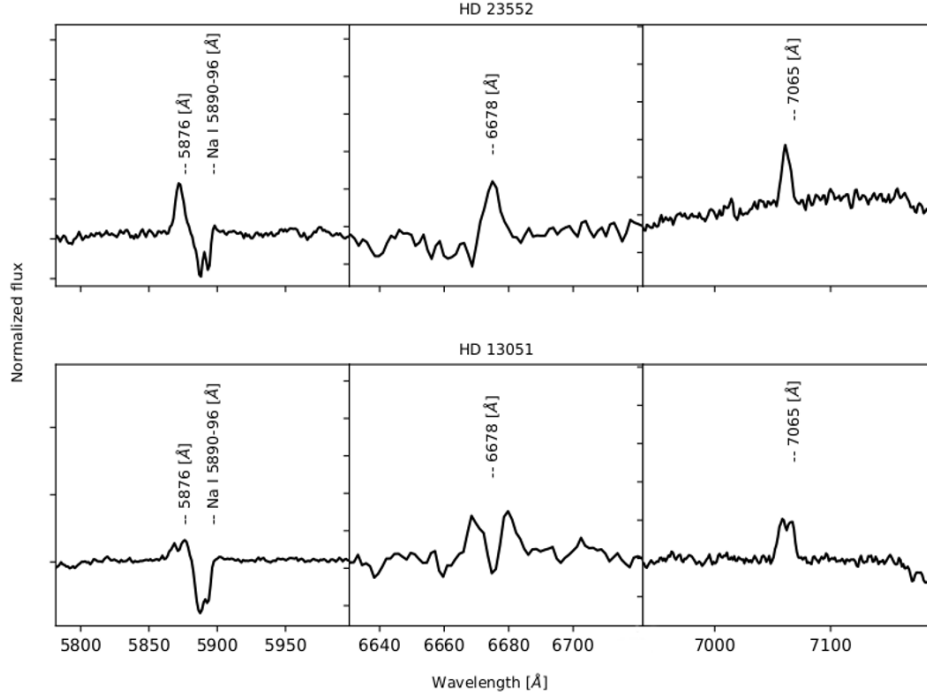


Figure 6. He I emission line profiles for the program stars HD 23552 and HD 13051. HD 23552 shows single-peaked emission of He I 5876, 6678 and 7065 Å lines, whereas double-peaked emission is visible in case of HD 13051.

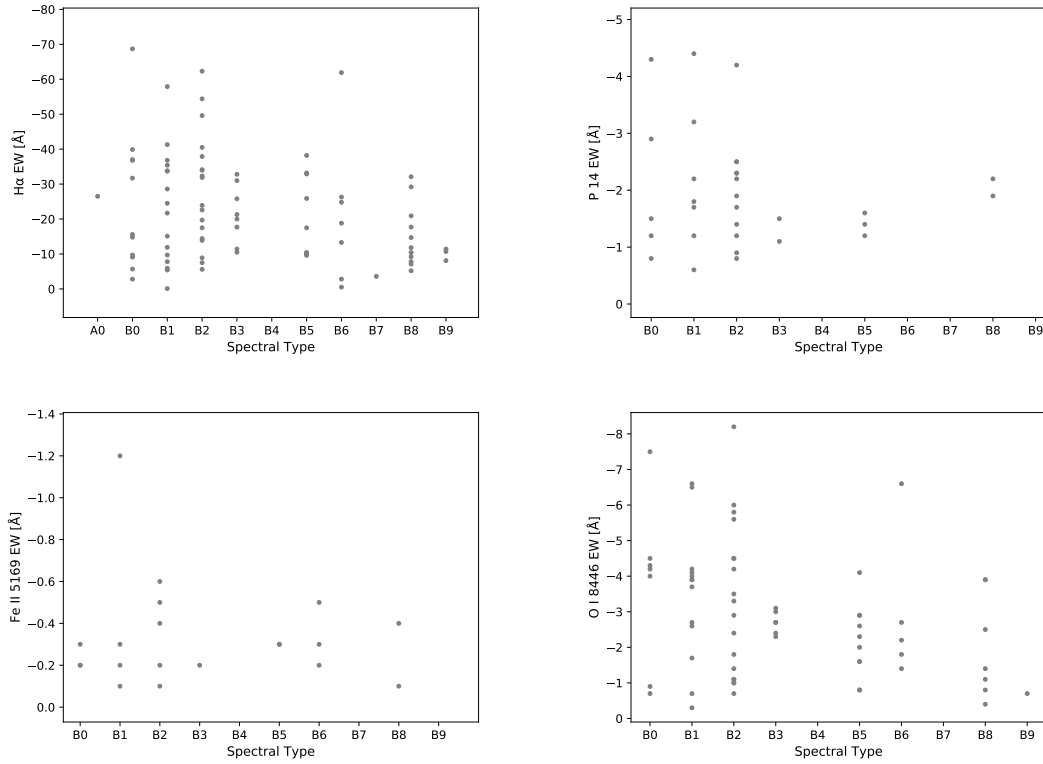


Figure 7. $H\alpha$, P14, Fe II 5169 Å and O I 8446 Å emission equivalent width of our program stars as a function of their spectral type. A clear spectral type dependency is observed for $H\alpha$, P14 and O I 8446 Å EW. It is noticed that the EW of $H\alpha$, P14 and O I 8446 Å emission lines attain a maximum value somewhere near B1–B2 types and gradually decrease towards late-types. Fe II 5169 Å EW also shows a trend of peaking near B1–B2 even if we remove the single data point lying near the -1.2 Å region in the respective plot.

3.3.8 Other prominent metallic emission lines

Other than oxygen lines, weak emission lines of SiII and MgII are occasionally present in CBe star spectra. Mathew & Subramaniam (2011) reported the occurrence of these lines in their sample of 152 cluster CBe stars. Study of these lines are almost absent in literature.

Among our program stars, 7 show both SiII 6347 and 6371 Å lines in emission, whereas in 16 cases both are present in absorption. In 5 other stars, only SiII 6347 Å line is visible in emission and only SiII 6371 Å line is seen in emission in two separate cases (HD 10516 and HD 277707). We also found that both MgII 7877 and 7896 Å lines are present in emission in 9 stars, while the star HD 45626 shows only MgII 7877 Å line in emission. On the contrary, only MgII 7896 Å line is observed in emission for the stars HD 19243 and HD 36376.

3.4 Balmer decrement studies

In CBe stars, relative emission strengths of Balmer emission lines is a function of the electron temperature and density in their disc. The flux ratios for the strongest emission lines visible in CBe star optical spectra are known as Balmer decrements. Thus, Balmer decrement is defined as

$$D_{34} = F(H\alpha)/F(H\beta) \quad (1)$$

$$D_{54} = F(H\gamma)/F(H\beta) \quad (2)$$

Here, D_{34} and D_{54} are usually quantified with respect to the emission strength (i.e. flux) of the $H\beta$ line, $F(H\beta)$. Primarily for the analysis of electron temperature and density in CBe star disc, people consider the values of D_{34} and D_{54} which are the flux ratios of $H\alpha$ and $H\gamma$ to $H\beta$, respectively. The corresponding line flux i.e. $F(H\alpha/H\beta)$ and $F(H\gamma/H\beta)$ are obtained by multiplying the continuum flux (F_C) ratio, i.e. $F_C(H\alpha/H\beta)$ and $F_C(H\gamma/H\beta)$ to the corrected equivalent width ratio, i.e. $EW(H\alpha/H\beta)$ and $EW(H\gamma/H\beta)$. Hence, the above equations can be expressed in more general form as:

$$(D_{34})_o = EW(H\alpha/H\beta) \times F_C(H\alpha/H\beta) \quad (3)$$

$$(D_{54})_o = EW(H\gamma/H\beta) \times F_C(H\gamma/H\beta) \quad (4)$$

where $(D_{34})_o$ and $(D_{54})_o$ are the observed D_{34} and D_{54} , respectively. We have used the above general formulae adopted from Dachs et al. (1990) for calculating D_{34} and D_{54} for our program stars.

Most of the earlier works on Balmer decrement of CBe stars were focussed on the study of D_{34} in field stars. Empirical studies dealing with Balmer decrement in CBe stars were carried out by Karpov (1934), Burbidge & Burbidge (1953) and Briot (1971, 1981). Since these were entirely based on observed emission line intensities through photographic spectrograms, the obtained results will most likely suffer from problems related to photographic intensity calibration (Dachs et al. 1990). Rojas & Herman (1958) found a variation of the $H\alpha : H\beta$ ratio with the temperature of the underlying star by studying their sample of 17 stars between B0 - B9 spectral types. They obtained the D_{34} value for these stars to be ranging between 2.2 to 4.2.

Some other studies (e.g. Dachs et al. (1990); Pottasch (1961); Burbidge & Burbidge (1955)) suggested that the electron density in

CBe star discs range between $10^{12} - 2 \times 10^{13} \text{ cm}^{-3}$. Furthermore, disc properties of CBe stars were investigated by Balmer decrement studies of 6 CBe shell stars (Kogure et al. 1978) and for the pole-on CBe star HR 5223 (Dachs et al. 1984). Dachs et al. (1990) determined the D_{34} and D_{54} values for 26 bright CBe stars and found the values of D_{34} to range within 1.2 to 3.2, while D_{54} ranging between 0.4 to 1.0. They calculated that for non-shell CBe stars, the mean electron density in the discs of their program stars not to be exceeding 10^{12} cm^{-3} . Mathew et al. (2012a) estimated the electron density for the star X Per to be within $10^{11} - 10^{13} \text{ cm}^{-3}$. This implies that CBe star envelopes are optically thick where the average electron density (n_e) is significantly larger than what is found in the nebular regions.

We presently know that the primary parameter which governs the D_{34} and D_{54} values is the electron density of the disc (Dachs et al. 1990). From the theoretical calculations of Hummer & Storey (1987), it is shown that $D_{34} \sim 2.7$ for case B hydrogen nebulae of low-density. Similarly the theoretical value for $D_{54} = 0.8$ is given by Storey & Hummer (1995). Case B condition is predicted to prevail in static, low-density regions having spherical shape such as planetary nebulae. These regions are generally modelled assuming them to be opaque in Lyman continuum, but transparent at larger wavelengths, while being excited, heated and photoionized by radiation coming from a hot, central star. Such a scenario, termed as case B condition was defined in the pioneering work of Baker & Menzel (1938) and later in follow-up studies, particularly by Brocklehurst (1971) which extends to slightly higher densities.

3.4.1 Estimation of D_{34} and D_{54} values

In this study, we estimated the D_{34} values for 105 and D_{54} values for 96 of our program stars, the largest sample used till date to study the Balmer decrement in CBe stars. D_{54} is calculated for those cases where $H\gamma$ is also present in emission along with $H\alpha$ and $H\beta$. The resulting values are listed in Table 4.

$H\alpha$ is observed in absorption for one of our star, HD 60855 (marked in bold in Table 4). In case of 5 other program stars (BD+10 2133, HD 10516, HD 277707, HD 51480 and HD 61224) we could not confirm the spectral types from the literature (marked with star in Table 4). Also, Grism 7 spectra is not available for the stars HD 45726 and HD 58343 (marked with asterisk in Table 4), thus $H\beta$, $H\gamma$ lines being not visible. Hence, we omitted these stars from Balmer decrement calculation. Moreover, while re-estimating the A_V values for our program stars, we found that three stars, namely HD 53367, BD-05 1318 and V615 Cas are classified as a Herbig Ae/Be star, a variable X-ray source and a high mass X-ray binary, respectively. These 3 stars exhibit high A_V values, which are shown in Table 2. So these 3 stars are also omitted from the Balmer decrement calculation.

The method we followed to estimate the D_{34} and D_{54} values is described below:

- At first, we measured the equivalent widths of $H\alpha$, $H\beta$ and $H\gamma$ lines for all our stars (shown in Table 4), irrespective of whether they are in emission or in absorption.
- Next, we identified the synthetic spectra corresponding to each spectral type (B0 - A0) using the Kurucz model (Kurucz 1993). For this purpose we need the effective temperature of the CBe star (T_{eff}), which is identified from Pecaut & Mamajek (2013) for each spectral type. We also adopted solar metallicity (Fe/H) and log g value as 4.5 (for Main Sequence stars).

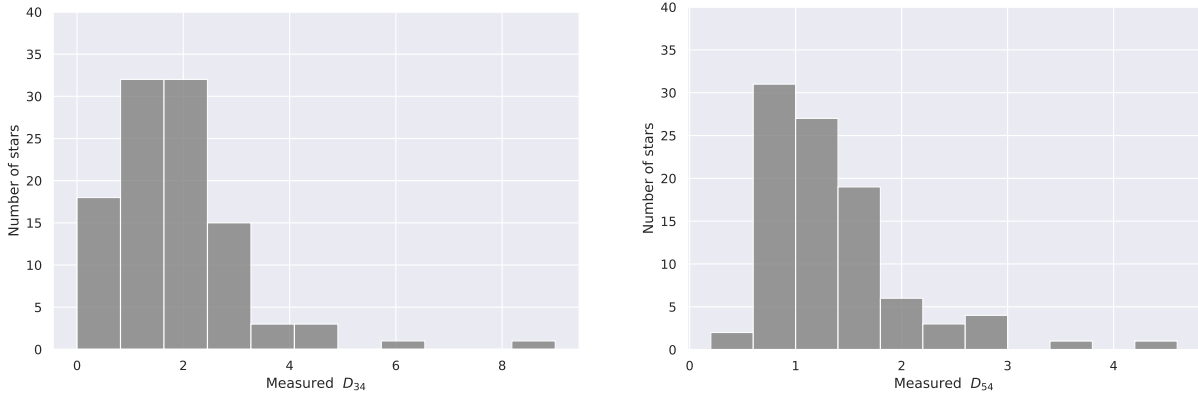


Figure 8. D_{34} and D_{54} distribution for our program stars. Among 105 stars for which we estimated D_{34} values, 19 ($\approx 20\%$) show $D_{34} \geq 2.7$. However, D_{54} for our stars mostly range between 0.2 and 1.5 ($\approx 70\%$). Only 19 stars exhibit $D_{34} < 1.0$, whereas $D_{54} > 1.5$ in 27 cases.

- Then, we measured the absorption component of $H\alpha$, $H\beta$ and $H\gamma$ lines from the synthetic spectra for each spectral type (B0 - A0). The absorption EW is added to the emission EW to obtain the net line EW since the emission line appears after filling in the absorption trough.

- Further, we determined the continuum flux (F_C) corresponding to $H\alpha$, $H\beta$ and $H\gamma$ lines for each spectral type from Kurucz synthetic spectra. We, thereby obtained the corresponding line flux i.e. $F(H\alpha/H\beta)$ by multiplying the continuum flux (F_C) ratio to the corrected equivalent width ratio (using equations 3 and 4). This gives the observed D_{34} and D_{54} values for each star.

- Next step is to correct the D_{34} and D_{54} values for extinction. A_V for 83 of our program stars are estimated using the newly available data from Gaia DR2. A_V estimated in the present study is used for flux correction.

- The corrected D_{34} and D_{54} values, i.e. $(D_{34})_c$ and $(D_{54})_c$ are calculated using the following relations:

$$(D_{34})_c = 10^{-(A(H\alpha)-A(H\beta))/2.5} \times (D_{34})_o \quad (5)$$

$$(D_{54})_c = 10^{-(A(H\gamma)-A(H\beta))/2.5} \times (D_{54})_o \quad (6)$$

Here, the extinction values at $H\alpha$, $H\beta$ and $H\gamma$ is determined from the parameterized, seventh-order polynomial fit to the interstellar extinction presented in Cardelli et al. (1989). This method of deriving the extinction at $\text{O I } 7774 \text{ \AA}$ and 8446 \AA lines have already been explored successfully by Mathew et al. (2012b). We estimated $A(H\alpha) = 0.8223A_V$, $A(H\beta) = 1.1881A_V$ and $A(H\gamma) = 1.3426A_V$. So, equivalently, $A(H\alpha)-A(H\beta) = -0.3659 \times A_V$ and $A(H\gamma)-A(H\beta) = 0.1561 \times A_V$ with a ratio of total-to-selective extinction, $R_V = 3.1$.

Names of the program stars are shown in column 1 of Table 4. Measured EW of $H\alpha$, $H\beta$, $H\gamma$ lines are listed in columns 2 to 4. Likewise, EW of $H\alpha$, $H\beta$, $H\gamma$ lines corrected for the influence of the underlying stellar absorption are shown in columns 5 to 7. Columns 8 and 9 present our estimated Balmer decrements, i.e. $(D_{34})_c$ and $(D_{54})_c$ values.

Data obtained from Column 8 of Table 4 shows that D_{34} for our program stars range between 0.1 and 9.0. Among 105 stars, 19 ($\approx 20\%$) show $D_{34} \geq 2.7$. The lowest and highest D_{34} values of 0.1 and 9.0 are obtained for HD 61205 and HD 251726, respectively.

We also noticed that 19 other stars exhibit $D_{34} < 1.0$, most of them showing weak emission with $H\alpha \text{ EW} < -5 \text{ \AA}$. The corresponding D_{54} values mostly range between 0.2 and 1.5 ($\approx 70\%$), clustering somewhere near 0.8 – 1.0 (column 9 of Table 4). However, in 27 cases $D_{54} \geq 1.5$ with one star, HD 251726 showing D_{54} as high as 4.6. The star HD 33461 shows $D_{54} = 0.2$, the least D_{54} value measured for our sample. Fig. 8 shows the distribution of D_{34} and D_{54} for our program stars.

Comparing with literature, we find that Dachs et al. (1990) reported D_{34} to lie within 1.2 - 3.2 for their sample of 26 southern early-type Be stars. However, D_{54} for their case range within 0.4 - 1.0, clustering near 0.7. On the contrary, Slettebak et al. (1992) obtained D_{34} for 41 CBe stars to range between 2.05 - 5.7, while D_{54} being always less than 1.0. Both the previous authors also noticed that on an average, weak $H\alpha$ emission ($H\alpha \text{ EW} < -25 \text{ \AA}$) is usually characterized by flat Balmer decrements ($D_{34} < 2.0$, $D_{54} > 0.6$). Our study could not confirm any such trend which is evident from Table 4.

Our result for D_{34} fairly agrees with Slettebak et al. (1992) and Dachs et al. (1990), although the range of our D_{34} is larger. This is possibly due to the larger number of stars for our sample. We found that 19 of our program stars show $D_{34} \geq 2.7$, implying that the disc for these stars are optically thick in nature. But our result does not match for D_{54} . The different range of D_{34} and D_{54} values obtained in our study might be due to the fact that we considered A_V values for calculating the Balmer decrements in our case. This may not have been done by previous authors. Moreover, we estimated D_{34} for all 20 weak emitters also which show $H\alpha \text{ EW} < -5 \text{ \AA}$.

3.4.2 Epoch-wise variation of D_{34}

Apart from looking into the $H\alpha$ line, the transient nature of CBe star discs can be identified by studying the epoch-wise variation of estimated D_{34} values of those stars where repeated observations are done. For our program stars where previous estimations of D_{34} are available (at least two), we compared our estimated D_{34} values to those obtained by other authors.

We found that only 10 of our program stars have at least two sets of observations for D_{34} including our estimations. Only one among them (HR 2142) has three observations for D_{34} . Fig. 9 demonstrates the variation of D_{34} as observed by us and previous authors. It is seen that our value of D_{34} is lower than that of previous authors

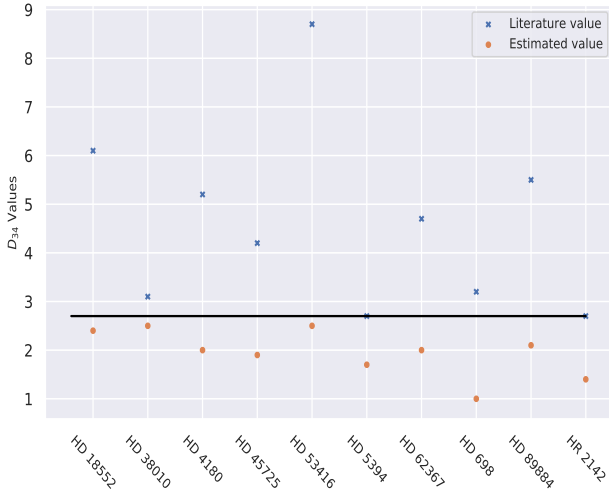


Figure 9. Variation of D_{34} in 10 of our program stars as observed by us and previous authors. The black line indicates the cutoff value 2.7, adopted from Hummer & Storey (1987), which is assumed to distinguish between an optically thin and thick region that prevails in case B condition defined by Baker & Menzel (1938) and later by Brocklehurst (1971).

(e.g. Dachs et al. (1990), Briot (1971), Rojas & Herman (1958), Burbidge & Burbidge (1953), Karpov (1934)) in every case.

The epoch-wise variation study of D_{34} for 10 of our program stars certainly imply that the optical thickness in the discs of these stars is changing within a timescale of years to decades, which may result in the disc transient nature.

4 SUMMARY

In this paper, we studied the major emission lines for 115 field CBe stars in the wavelength range of 3800 - 9000 Å selected from the catalogue of Jaschek & Egret (1982). According to the best of our knowledge, this is the first study where near simultaneous spectra covering the whole spectral range of 3800 - 9000 Å has been studied for over 100 field CBe stars. We, therefore, produce an atlas of emission lines for CBe stars which will be a valuable resource for researchers involved in CBe star research. The main results obtained from our study are summarized below:

- We re-estimated the extinction parameter (A_V) for 83 of our sample stars using the newly available data from Gaia DR2. For the rest 35 cases, we obtained the A_V values from literature. The estimated A_V values are used for extinction correction in the analysis of Balmer decrement for our program stars. Hence, we suggest that A_V is of much importance and has to be taken into account for the analysis of CBe star properties.

- We measured the Balmer decrement, i.e. D_{34} values for 105 and D_{54} values for 96 of our program stars, the first work till date to study the Balmer decrement for a sample of more than 100 CBe stars. D_{34} in our sample ranges between 0.1 and 9.0, whereas the corresponding D_{54} values mostly ($\approx 70\%$) range between 0.2 and 1.5, clustering somewhere near 0.8 - 1.0. Among 105 stars, 19 ($\approx 20\%$) show $D_{34} > 2.7$. Considering the effect of A_V in our sample stars, our result implies that CBe star disc are generally optically thick in nature for some stars. Moreover, epoch-wise variation study

of D_{34} for 10 of our program stars imply that the optical thickness in the discs of these stars is changing within a timescale of years to decades.

- Majority of our program stars ($\approx 60\%$, 68) show $H\alpha$ in normal, single-peaked emission, with the $H\alpha$ EW ranging within -0.5 to -72.7 Å for our sample. Among these, we identified 20 weak emitters with $H\alpha$ EW < -5.0 Å, whereas only one star, HD 60855, exhibits $H\alpha$ in absorption - indication of the disc-less state. Our analysis also suggests that the $H\alpha$ EW values in CBe stars are mostly lower than -40 Å.

- We analyzed the CaII triplet emission lines observed in $\approx 15\%$ (17) cases for our program stars. By exploring various formation regions of CaII emission lines around the circumstellar disc of CBe stars, we suggest the possibility that CaII triplet emission can originate either (1) in the circumbinary disc or, (2) from the cooler outer regions of the disc which might not be isothermal in nature.

- Paschen lines are present in emission in $\approx 40\%$ (47) stars of our sample, 39 among them belonging to spectral types earlier than B5 which is in agreement with Briot (1981). In 11 cases, CaII emission lines are found to be blended along-with. We also observed that the emission strength of Paschen lines gradually decrease from P12 to the series limit in all our program stars, irrespective of the spectral type. In our study, this trend in the emission strength distribution is used for deblending the Paschen emission components from CaII triplet emission lines.

- FeII emission lines are observed in $\approx 83\%$ (95) of our program stars, in agreement with Mathew & Subramaniam (2011). Around 85% of our stars showing FeII lines in emission have spectral types earlier than B6, thus supporting Andriolat et al. (1988). Moreover, we noticed that a threshold value (~ -10 Å) of $H\alpha$ EW is necessary for FeII emission to become visible in CBe stars. OI 8446 and 7772 Å emission lines are present in $\approx 57\%$ (66) and $\approx 38\%$ (44) of our program stars, respectively. From our analysis, it appears that the emission strength of $H\alpha$, P14, FeII 5169 Å and OI 8446 Å is more in early B-type stars.

- Furthermore, we identified HeI 5876, 6678 and 7065 Å emission lines in $\approx 11\%$ (13) stars, 12 among them belonging to B3 type or earlier. This indicates that hotter CBe stars of earlier spectral types might have higher disc temperature, thus showing HeI lines.

ACKNOWLEDGEMENTS

We would like to thank the Science & Engineering Research Board (SERB) under the Government of India for supporting our research. We also thank the Center for research, CHRIST (Deemed to be University), Bangalore, India. Moreover, we thank the staff of the Indian Astronomical Observatory (IAO), Ladakh for taking the observations using the HCT situated at Hanle. This work has used the Gaia DR2 data to re-estimate the extinction parameters for our program stars. Hence, we express our gratitude to the Gaia collaboration for providing the data. We also thank the SIMBAD database and the online VizieR library service for helping us in literature survey and obtaining relevant data. Lastly, we acknowledge the anonymous reviewer for providing constructive comments which helped in considerable modification of the manuscript.

DATA AVAILABILITY

The data underlying this article will be shared on reasonable request to the corresponding author.

REFERENCES

- Andrillat Y., Fehrenbach C., 1982, in Jaschek M., Groth H. G., eds, IAU Symposium Vol. 98, Be Stars. pp 135–139
- Andrillat Y., Houziaux L., 1967, Publications of the Observatoire Haute-Provence, **9**, 107
- Andrillat Y., Jaschek M., Jaschek C., 1988, A&AS, **72**, 129
- Apparao K. M. V., Tarafdar S. P., 1994a, *ApJ*, **420**, 803
- Apparao K. M. V., Tarafdar S. P., 1994b, *ApJ*, **420**, 803
- Arcos C., Jones C. E., Sigut T. A. A., Kanaan S., Curé M., 2017, *ApJ*, **842**, 48
- Arias M. L., Zorec J., Cidale L., Ringuelet A. E., Morrell N. I., Ballereau D., 2006, A&A, **460**, 821
- Bahng J. D. R., Hendry E., 1975, *PASP*, **87**, 137
- Bailer-Jones C. A. L., Rybizki J., Fouesneau M., Mantelet G., Andrae R., 2018, *AJ*, **156**, 58
- Baker J. G., Menzel D. H., 1938, *ApJ*, **88**, 52
- Ballereau D., Chauville J., Zorec J., 1995, A&AS, **111**, 457
- Banerjee D. P. K., Rawat S. D., Janardhan P., 2000, A&AS, **147**, 229
- Barnsley R. M., Steele I. A., 2013, A&A, **556**, A81
- Bhat S. S., Paul K. T., Subramaniam A., Mathew B., 2016, *Research in Astronomy and Astrophysics*, **16**, 76
- Borre C. C., et al., 2020, A&A, **635**, A140
- Bowen I. S., 1947, *PASP*, **59**, 196
- Briot D., 1971, A&A, **11**, 57
- Briot D., 1981, A&A, **103**, 5
- Brocklehurst M., 1971, *MNRAS*, **153**, 471
- Burbidge G. R., Burbidge E. M., 1953, *ApJ*, **118**, 252
- Burbidge E. M., Burbidge G. R., 1955, *The Observatory*, **75**, 256
- Carciofi A. C., Bjorkman J. E., 2006, *ApJ*, **639**, 1081
- Carciofi A. C., Bjorkman J. E., 2008, *ApJ*, **684**, 1374
- Carciofi A. C., Bjorkman J. E., Otero S. A., Okazaki A. T., Štefl S., Rivinius T., Baade D., Haubois X., 2012, *ApJ*, **744**, L15
- Cardelli J. A., Clayton G. C., Mathis J. S., 1989, *ApJ*, **345**, 245
- Catanzaro G., 2013, A&A, **550**, A79
- Chalabaev A. A., Maillard J. P., 1985, *ApJ*, **294**, 640
- Chen P. S., Liu J. Y., Shan H. G., 2016, *MNRAS*, **463**, 1162
- Chojnowski S. D., et al., 2018, *ApJ*, **865**, 76
- Clark J. S., Steele I. A., 2000, A&AS, **141**, 65
- Cox A. N., 2000, *Allen's astrophysical quantities*. Springer New York
- Dachs J., Hanuschik R., Kaiser D., 1984, *Mitteilungen der Astronomischen Gesellschaft Hamburg*, **62**, 268
- Dachs J., et al., 1986, A&AS, **63**, 87
- Dachs J., Rohe D., Loose A. S., 1990, A&A, **238**, 227
- Dachs J., Hummel W., Hanuschik R. W., 1992, A&AS, **95**, 437
- Fabregat J., et al., 1992, A&A, **259**, 522
- Gontcharov G. A., 2012, *Astronomy Letters*, **38**, 87
- Granada A., Arias M. L., Cidale L. S., Mennickent R. E., 2011, in Neiner C., Wade G., Meynet G., Peters G., eds, IAU Symposium Vol. 272, Active OB Stars: Structure, Evolution, Mass Loss, and Critical Limits. pp 392–393, doi:10.1017/S1743921311010878
- Green G. M., Schlafly E., Zucker C., Speagle J. S., Finkbeiner D., 2019, *ApJ*, **887**, 93
- Hanuschik R. W., 1986, A&A, **166**, 185
- Hanuschik R. W., 1987, A&A, **173**, 299
- Hanuschik R. W., 1988, A&A, **190**, 187
- Hanuschik R. W., 1994, in Balona L. A., Henrichs H. F., Le Contel J. M., eds, IAU Symposium Vol. 162, Pulsation; Rotation; and Mass Loss in Early-Type Stars. p. 265
- Hanuschik R. W., Hummel W., Sutorius E., Dietle O., Thimm G., 1996, A&AS, **116**, 309
- Hiltner W. A., 1947, *ApJ*, **105**, 212
- Hummer D. G., Storey P. J., 1987, *MNRAS*, **224**, 801
- Ivanova D. V., Sakhibullin N. A., Shimanskii V. V., 2004, *Astronomy Reports*, **48**, 476
- Jaschek M., Egret D., 1982, in Jaschek M., Groth H. G., eds, IAU Symposium Vol. 98, Be Stars. p. 261
- Jaschek C., Jaschek M., 1983, A&A, **117**, 357
- Jaschek M., Hubert-Delplace A. M., Hubert H., Jaschek C., 1980, A&AS, **42**, 103
- Jaschek M., Jaschek C., Andrillat Y., 1993, A&AS, **97**, 781
- Jones C. E., Sigut T. A. A., Marlborough J. M., 2004, *MNRAS*, **352**, 841
- Karpov B. G., 1934, PhD thesis, UNIVERSITY OF CALIFORNIA, BERKELEY.
- Kitchin C. R., Meadows A. J., 1970, *Ap&SS*, **8**, 463
- Klement R., et al., 2019, *ApJ*, **885**, 147
- Kogure T., Hirata R., Asada Y., 1978, *PASJ*, **30**, 385
- Koubský P., Ak H., Harmanec P., Yang S., Božić H., 2004, in Kurtz D. W., Pollard K. R., eds, Astronomical Society of the Pacific Conference Series Vol. 310, IAU Colloq. 193: Variable Stars in the Local Group. p. 387
- Koubský P., Kotková L., Votruba V., 2011, in Journal of Physics Conference Series. p. 012026, doi:10.1088/1742-6596/328/1/012026
- Koubský P., et al., 2012, arXiv e-prints, p. arXiv:1205.2259
- Kurucz R. L., 1993, in Dworetzky M. M., Castelli F., Faraggiana R., eds, Astronomical Society of the Pacific Conference Series Vol. 44, IAU Colloq. 138: Peculiar versus Normal Phenomena in A-type and Related Stars. p. 87
- Kwan J., Fischer W., 2011, *MNRAS*, **411**, 2383
- Lee U., Osaki Y., Saio H., 1991, *MNRAS*, **250**, 432
- Lennon D. J., Dufton P. L., 1989, A&A, **225**, 439
- Levenhagen R. S., Diaz M. P., Amôres E. B., Leister N. V., 2020, arXiv e-prints, p. arXiv:2009.06493
- Mathew B., Subramaniam A., 2011, Bulletin of the Astronomical Society of India, **39**, 517
- Mathew B., Subramaniam A., Bhatt B. C. r., 2008, *MNRAS*, **388**, 1879
- Mathew B., Banerjee D. P. K., Naik S., Ashok N. M., 2012a, *MNRAS*, **423**, 2486
- Mathew B., Banerjee D. P. K., Subramaniam A., Ashok N. M., 2012b, *ApJ*, **753**, 13
- McGill M. A., Sigut T. A. A., Jones C. E., 2013, *ApJS*, **204**, 2
- Meilland A., et al., 2007, A&A, **464**, 59
- Mennickent R. E., Sabogal B., Granada A., Cidale L., 2009, *PASP*, **121**, 125
- Mennickent R. E., Rivinius T., Cidale L., Soszyński I., Fernández-Trincado J. G., 2018, *PASP*, **130**, 094204
- Mermilliod J. C., 1982, A&A, **109**, 48
- Moto'oka K., Itoh Y., 2013, *Research in Astronomy and Astrophysics*, **13**, 1189
- Norton A. J., et al., 1991, *MNRAS*, **253**, 579
- Osterbrock D. E., Ferland G. J., 2006, *Astrophysics of gaseous nebulae and active galactic nuclei*. University Science Books
- Paul K. T., Subramaniam A., Mathew B., Mennickent R. E., Sabogal B., 2012, *MNRAS*, **421**, 3622
- Paul K. T., Shruthi S. B., Subramaniam A., 2017, *Journal of Astrophysics and Astronomy*, **38**, 6
- Pecaut M. J., Mamajek E. E., 2013, *ApJS*, **208**, 9
- Peton A., 1972, A&A, **18**, 106
- Polidan R. S., Peters G. J., 1976, in Slettebak A., ed., IAU Symposium Vol. 70, Be and Shell Stars. p. 59
- Porter J. M., Rivinius T., 2003, *PASP*, **115**, 1153
- Pottasch S. R., 1961, *Annales d'Astrophysique*, **24**, 159
- Rivinius T., Carciofi A. C., Martayan C., 2013, A&ARv, **21**, 69
- Rojas H., Herman R., 1958, *8eme Colloque Intern. d'Astrophys. a Liege*, **20**, 198
- Schootemeijer A., Götzberg Y., de Mink S. E., Gies D., Zapartas E., 2018, A&A, **615**, A30
- Shokry A., et al., 2018, A&A, **609**, A108
- Sigut T. A. A., Jones C. E., 2007, *ApJ*, **668**, 481
- Siviero A., Munari U., 2003, in Corradi R. L. M., Mikolajewska J., Mahoney T. J., eds, Astronomical Society of the Pacific Conference Series Vol.

- 303, Symbiotic Stars Probing Stellar Evolution. p. 167
- Slettebak A., 1982, [ApJS](#), **50**, 55
- Slettebak A., Collins George W. I., Truax R., 1992, [ApJS](#), **81**, 335
- Smith M. A., Cohen D. H., Hubeny I., Plett K., Basri G., Johns-Krull C. M., MacFarlane J. J., Hirata R., 1997, [ApJ](#), **481**, 467
- Smith M. A., Lopes de Oliveira R., Motch C., 2017, [MNRAS](#), **469**, 1502
- Steele I. A., Clark J. S., 2001, [A&A](#), **371**, 643
- Stevens D. J., Stassun K. G., Gaudi B. S., 2017, [AJ](#), **154**, 259
- Storey P. J., Hummer D. G., 1995, VizieR Online Data Catalog, [p. VI/64](#)
- Struve O., 1931, [ApJ](#), **74**, 225
- Swihart S. J., Garcia E. V., Stassun K. G., van Belle G., Mutterspaugh M. W., Elias N., 2017, [AJ](#), **153**, 16
- Tarafdar S. P., Apparao K. M. V., 1994, [A&A](#), **290**, 159
- Varga J., et al., 2018, [A&A](#), **617**, A83
- Wang S., Chen X., de Grijs R., Deng L., 2018, VizieR Online Data Catalog, [p. J/ApJ/852/78](#)
- Zhang P., Chen P. S., Yang H. T., 2005, [New Astron.](#), **10**, 325
- Zorec J., Briot D., 1997, [A&A](#), **318**, 443

This paper has been typeset from a $\text{\TeX}/\text{\LaTeX}$ file prepared by the author.

Table 1. List of our program CBe stars and the log of observations.

Be star	Alias	V mag	Sp.type	date of observation dd/mm/yyyy	Exp. time (s)
AS 1	BD+62 11	9.6	B5V	03-12-2007	120
				02-12-2008	240
AS 105	BD+37 1292	9.2	B3Vpe	12-01-2008	300
AS 52	BD+61 371	11	B3IIep	26-02-2008	360
BD-05 1318	V1230 Ori	9.7	B8IV-Ve	01-12-2008	180
BD+10 2133	BD+10 2133	10.5	Be	28-12-2007	200
BD+55 81	BD+55 81	10	B1.5Vnne	03-12-2007	120
				02-12-2008	300
BD+59 334	BD+59 334	10.6	B0Ve	16-12-2008	300
BD+60 307	BD+60 307	10.5	B2Ve	16-12-2008	300
BD+60 368	ALS 6797	10.5	B1IIIe	16-12-2008	300
BD+62 287	BD+62 287	9.1	B8Ve	16-12-2008	240
BD+62 292	BD+62 292	10.6	B1ep	16-12-2008	300
BD+62 300	BD+62 300	9.9	B1Vep	16-12-2008	180
CD-22 4761	CD-22 4761	10.2	B0:nne	22-12-2008	300
HD 10516	Phi Per	4.1	B2V/BIV	16-12-2007	5
				03-12-2008	2
HD 109387	Kappa Dra	3.9	B6IIIpe	04-01-2009	120
HD 12302	BD+58 356	8.1	B1V	27-12-2007	240
HD 12856	BD+56 429	8.6	B0	26-02-2008	60
HD 12882	V782 Cas	7.6	B2.5III:[n]e+	06-01-2009	60
HD 13051	V351 Per	8.6	B1IV	06-01-2009	120
HD 13429	BD+54 483	9.2	B3V	06-01-2009	240
HD 144	10 Cas	5.6	B9III	02-12-2007	15
				06-01-2009	10
HD 15238	V529 Cas	8.5	B5V	11-01-2008	120
HD 18552	HR 894	6.1	B8V	27-12-2007	10
HD 18877	BD+59 589	8.4	B7II-III	27-12-2007	120
HD 19243	V801 Cas	6.5	B1V	27-12-2007	10
HD 20017	BD+48 870	7.9	B5V	27-12-2007	120
HD 20134	BD+59 625	7.5	B2.5IV-V	27-12-2007	60
HD 20336	BK Cam	4.7	B2.5V	27-12-2007	5
HD 20340	BD-17 631	7.9	B3V	27-12-2007	120
HD 21212	BD+61 587	8.3	B2V	27-12-2007	120
HD 21455	HR 1047	6.2	B6V	27-12-2007	10
HD 21641	BD+47 846	6.8	B9V	27-12-2007	30
HD 218393	KX And	7	Bpe	03-12-2008	60
HD 22780	HR 1113	5.5	B7V	20-12-2008	120
HD 232590	BD+54 448	8.6	B1.5III	27-12-2007	120
HD 23302	17 Tau	3.7	B6III	20-12-2008	5
				05-01-2009	2
HD 23552	HR 1160	6.2	B8V	05-01-2009	10
HD 23630	Eta Tau	2.9	B7III	20-12-2008	5
				05-01-2009	3
HD 236935	BD+57 469	9.4	B1Vne	26-02-2008	240
HD 236940	BD+55 489	9.6	B1Ve	04-01-2009	240
HD 237056	BD+57 681	8.9	B0.5ep	27-12-2007	240
HD 237060	BD+58 554	9.2	B9Ve	27-12-2007	240
HD 237091	BD+59 612	8.9	B1Vnnep	27-12-2007	240
HD 237118	BD+59 632	9.4	B6Ve	27-12-2007	240
HD 237134	BD+59 647	9.5	B5Ve	27-12-2007	240
HD 23862	28 Tau	5	B8IV	20-12-2008	20
				05-01-2009	10
HD 244894	BD+27 797	10.1	B1III-IVpe	01-12-2008	180
HD 249695	BD+30 1071	9.2	B1Vnnep	04-01-2009	180
HD 251726	BD+19 1210	9.3	B1Ve	12-01-2008	300
HD 25487	RW Tau	8.2	B8V	01-12-2008	120
HD 25940	c Per	4	B3V	20-12-2008	60
HD 259597	MWC 149	8.6	B0.5Vnne	06-01-2009	120
HD 259631	MWC 810	9.6	B5	06-01-2009	240
HD 277707	MWC 484	10.4	Bpe	06-01-2009	300

Be star	Alias	V mag	Sp.type	date of observation dd/mm/yyyy	Exp. time (s)
HD 2789	BD+66 35	8.4	B3V	03-12-2007	80
				02-12-2008	180
HD 29441	V1150 Tau	7.6	B2.5V	20-12-2008	120
HD 29866	HR 1500	6.1	B8IV	20-12-2008	60
HD 33328	Iam Eri	4.3	B2IV	06-01-2009	10
HD 33357	SX Aur	8.6	B1V	06-01-2009	240
HD 33461	V415 Aur	7.8	B2V	06-01-2009	60
HD 35345	BD+35 1095	8.4	B1V	01-12-2008	60
HD 36012	V1372 Ori	7.2	B5V	01-12-2008	60
HD 36376	V1374 Ori	7.5	B8	01-12-2008	60
HD 36576	120 Tau	5.7	B2IV-V	01-12-2008	2
HD 37115	BD-05 1330	7.2	B6V	01-12-2008	30
HD 37657	V434 Aur	7.3	B3V	12-01-2008	300
HD 37806	BD-02 1344	7.9	A0	02-12-2008	30
HD 37967	V731 Tau	6.2	B2.5V	12-01-2008	10
HD 38010	V1165 Tau	6.8	B1V	12-01-2008	10
HD 38708	V438 Aur	8.1	B3	02-12-2008	120
HD 4180	Omi Cas	4.5	B5III	03-12-2007	5
				03-12-2008	2
HD 45542	Nu Gem	4.1	B6III	05-01-2009	10
HD 45626	BD-04 1534	9.3	B7	02-12-2008	180
HD 45725	beta Mon A	4.6	B3V	06-01-2009	20
HD 45726	beta Mon B	5.4	B2	06-01-2009	20
HD 45901	V725 Mon	8.9	B2Ve	06-01-2009	120
HD 45910	AX Mon	6.7	B2IIIpshev	06-01-2009	10
HD 46131	BD-22 1434	7.1	B4V	02-12-2008	60
HD 47359	BD+05 1340	8.9	B0.5Vpe	02-12-2008	120
HD 49330	V739 Mon	8.9	B0nnep	27-12-2007	120
HD 50658	BD+46 1203	5.9	B8IIIe	02-12-2008	5
HD 50696	BD+00 1691	8.9	B1e	02-12-2008	120
HD 50820	HR 2577	6.3	B3IVe	01-12-2008	10
HD 50868	V744 Mon	7.9	B2Vne	26-02-2008	60
HD 51193	V746 Mon	8.1	B1Vnn	26-02-2008	120
HD 51354	QY Gem	7.2	B3ne	02-12-2008	60
HD 51480	V644 Mon	6.9	Ape	01-12-2008	30
HD 53085	V749 Mon	7.2	B8e	12-01-2008	300
HD 53367	BD-10 1848	7	B0IVe	05-01-2009	60
HD 53416	BD+14 1558	6.8	B8IVe	01-12-2008	10
HD 5394	Gamma Cas	2.4	B0.5IV	02-12-2007	15
				26-02-2008	0.5
				03-12-2008	0.5
HD 55439	BD-09 1905	8.6	B2Ve	01-12-2008	120
HD 55606	BD-01 1603	9	B1Vnnpe	01-12-2008	120
HD 55806	BD+03 1613	9.1	B9esh	11-01-2008	180
				26-02-2008	60
HD 58050	OT Gem	6.5	B2Ve	11-01-2008	10
HD 58343	FW CMa	5.2	B3IVe	11-01-2008	5
HD 60260	BD-11 1994	9	B5e	11-01-2008	120
HD 60855	V378 Pup	5.7	B2Ve	11-01-2008	5
HD 61205	BD-11 1994	9.6	AOIV	22-12-2008	180
HD 61224	HR 2932	6.5	B8/B9IV	22-12-2008	90
HD 62367	BD-04 2062	7.1	B9	22-12-2008	90
HD 65079	BT CMi	7.8	B2Ve	04-01-2009	90
HD 698	BD+57 28	7.1	B5II	03-12-2007	60
				02-12-2008	30
HD 72043	BD-10 2546	8.8	B8e	04-01-2009	120
HD 89884	BD-17 3133	7.1	B5III	04-01-2009	90
HR 2142	HD 41335	5.3	B2V	02-12-2008	15
MWC 28	BD+57 515	9.8	B2pe	06-01-2009	240
MWC 3	BD+59 2829	9.9	B0IVnep	02-12-2007	100
				06-01-2009	120

Be star	Alias	V mag	Sp.type	date of observation dd/mm/yyyy	Exp. time (s)
MWC 5	BD+61 39	8.9	B0.5IV	03-12-2007	70
				02-12-2008	120
MWC 500	BD+35 1169	9.4	B1Vpe	01-12-2008	200
MWC 566	BD-11 2043	9.6	B	22-12-2008	120
MWC 667	BD+62 1	10.5	B2IV-Vpe	03-12-2007	120
				02-12-2008	240
				06-01-2009	420
MWC 669	BD+63 48	9.3	B1IIIInne	03-12-2007	180
				02-12-2008	300
MWC 672	BD+61 122	10.4	B2Vpe	03-12-2007	120
				02-12-2008	180
MWC 677	MWC 677	10.7	B2Vep	03-12-2007	150
				03-12-2008	300
MWC 678	MWC 678	9.9	B2Vnnep	03-12-2007	120
				03-12-2008	240
V615 Cas	LS I +61 303	10.8	B0Ve	04-01-2009	180

Table 2. Our adopted distance (in parsec) for 83 of our sample stars whose parallax values are available in Gaia DR2 (shown in columns 2 and 6) and their re-estimated A_V values are presented in columns 3 and 7. The associated errors for our adopted distance and re-estimated A_V values are also displayed. A_V obtained from the literature are presented in columns 4 and 8 for the respective stars.

Name	Distance (pc)	A_V mag	A_V (literature)	Name	Distance (pc)	A_V mag	A_V (literature)
AS 1	1990–137 ⁺¹⁵⁸	0 ± 0	1.2 ^a	HD 259597	1220–115 ⁺¹⁴¹	1.7 ± 0	1 ^c
AS 105	1110–71 ⁺⁸¹	0.1 ± 0	0.8 ^a	HD 259631	1405–90 ⁺¹⁰²	1.9 ± 0	0.6 ^a
AS 52	3575–401 ⁺⁵¹¹	0 ± 0	2.1 ^a	HD 277707	2161–302 ⁺⁴¹³	2.7 ± 0.2	1.5 ^c
BD+10 2133	1215–85 ⁺⁹⁹	0.6 ± 0.1	0 ^b	HD 2789	494–9 ⁺⁹	0.9 ± 0	1.8 ^a
BD+55 81	2169–170 ⁺²⁰¹	1.1 ± 0	0.9 ^c	HD 29441	737–35 ⁺³⁹	0.3 ± 0	0.6 ^a
BD+58 356	946–33 ⁺³⁶	1.3 ± 0.1	1.4 ^a	HD 29866	217–3 ⁺³	0.4 ± 0.1	0.5 ^b
BD+59 334	2413–158 ⁺¹⁸¹	2.6 ± 0	0.9 ^a	HD 33357	1444–111 ⁺¹³¹	0.9 ± 0	0.7 ^a
BD+60 307	2730–300 ⁺³⁸⁰	0.2 ± 0	2.1 ^a	HD 33461	1055–66 ⁺⁷⁶	0 ± 0	1.3 ^a
BD+60 368	3085–265 ⁺³¹⁸	1.1 ± 0.05	2.4 ^a	HD 35345	1168–78 ⁺⁸⁹	1.1 ± 0	1.1 ^a
BD+61 587	1083–44 ⁺⁴⁷	0.3 ± 0.3	2.4 ^a	HD 37657	749–42 ⁺⁴⁷	0 ± 0	0.6 ^a
BD+62 287	686–19 ⁺²⁰	0.1 ± 0	1.3 ^a	HD 37806	423–10 ⁺¹⁰	0 ± 0	0.3 ^e
BD+62 292	3216–319 ⁺³⁹⁵	1.1 ± 0	2.2 ^a	HD 37967	302–6 ⁺⁷	0.2 ± 0.1	0.6 ^b
BD+62 300	2655–199 ⁺²³³	0.9 ± 0.06	1.8 ^a	HD 38708	1191–80 ⁺⁹³	0 ± 0	0.5 ^a
BD-05 1318	429–11 ⁺¹²	4.6 ± 0.1	1.3 ^c	HD 45626	1657–122 ⁺¹⁴²	0 ± 0	0.6 ^a
CD-22 4761	3622–380 ⁺⁴⁷⁷	1.3 ± 0	2.2 ^c	HD 45901	2209–201 ⁺²⁴⁵	0.2 ± 0	1.6 ^a
HD 12882	921–29 ⁺³¹	0 ± 0	1.5 ^c	HD 45910	1086–51 ⁺⁵⁷	0 ± 0	1.4 ^a
HD 13051	2391–273 ⁺³⁵⁰	0.2 ± 0.02	1.2 ^a	HD 47359	1922–186 ⁺²²⁹	1.1 ± 0.1	1.6 ^a
HD 13429	1109–55 ⁺⁶¹	0.1 ± 0	0.9 ^a	HD 49330	1536–104 ⁺¹²¹	2 ± 0	1.6 ^a
HD 15238	639–15 ⁺¹⁵	0.5 ± 0	1.7 ^a	HD 50696	1255–100 ⁺¹¹⁸	0.1 ± 0	0.7 ^a
HD 18552	226–6 ⁺⁶	0.3 ± 0.1	0.2 ^a	HD 51193	1571–177 ⁺²²⁷	0.2 ± 0.04	0.9 ^a
HD 18877	459–9 ⁺⁹	0.5 ± 0	0.8 ^a	HD 51480	1301–133 ⁺¹⁶⁷	0 ± 0	1.4 ^c
HD 19243	928–129 ⁺¹⁷⁸	0.2 ± 0.02	1.3 ^b	HD 53367	130–12 ⁺¹⁵	5.3 ± 0.1	1.9 ^a
HD 20017	909–44 ⁺⁴⁸	0 ± 0	1.3 ^a	HD 55439	1285–119 ⁺¹⁴⁵	0.3 ± 0.1	0.9 ^c
HD 20134	609–16 ⁺¹⁷	0 ± 0	0.9 ^a	HD 55606	1090–43 ⁺⁴⁶	2.5 ± 0	0.7 ^a
HD 21455	169–2 ⁺¹	0.5 ± 0.1	0.5 ^a	HD 55806	885–38 ⁺⁴²	0.2 ± 0	0.6 ^a
HD 21641	174–2 ⁺²	0.8 ± 0.1	0.2 ^a	HD 60855	483–23 ⁺²⁶	0 ± 0	0.3 ^a
HD 218393	785–19 ⁺²⁰	0 ± 0	1.6 ^c	HD 61205	665–38 ⁺⁴³	0 ± 0	0.4 ^b
HD 22780	214–6 ⁺⁷	0 ± 0.1	0.2 ^f	HD 61224	497–12 ⁺¹³	0 ± 0	0.3 ^c
HD 232590	791–22 ⁺²³	0 ± 0	0.7 ^a	HD 65079	793–41 ⁺⁴⁶	0 ± 0	0.1 ^a
HD 23552	261–4 ⁺⁴	0 ± 0	0.4 ^a	HD 698	770–32 ⁺³⁵	0 ± 0	0.9 ^a
HD 236935	2460–195 ⁺²³¹	0.5 ± 0.03	1.7 ^a	HD 72043	1051–66 ⁺⁷⁵	0.4 ± 0	0.1 ^a
HD 236940	1928–149 ⁺¹⁷⁶	0.1 ± 0	1.1 ^a	HR 2142	467–33 ⁺³⁸	0 ± 0	0.5 ^a
HD 237056	975–42 ⁺⁴⁶	2.5 ± 0	2.5 ^a	MWC 28	2412–228 ⁺²⁸⁰	0 ± 0	1.4 ^a
HD 237060	637–12 ⁺¹²	0 ± 0	1.2 ^a	MWC 3	2530–196 ⁺²³⁰	1.8 ± 0	1.9 ^a

Name	Distance (pc)	A _V mag	A _V (literature)	Name	Distance (pc)	A _V mag	A _V (literature)
HD 237118	647–15 ⁺¹⁶	0.8 ± 0.06	0.9 ^a	MWC 5	2750–245 ⁺²⁹⁶	0.3 ± 0	1.3 ^a
HD 237134	671–19 ⁺²⁰	0.6 ± 0	1.7 ^a	MWC 500	1657–109 ⁺¹²⁶	1.3 ± 0	2 ^a
HD 244894	1973–149 ⁺¹⁷⁵	1.7 ± 0.08	1.8 ^a	MWC 566	3430–429 ⁺⁵⁵⁹	1 ± 0	1 ^c
HD 249695	1398–132 ⁺¹⁶²	1.5 ± 0	1 ^a	MWC 667	2893–210 ⁺²⁴⁵	0.2 ± 0.02	1.7 ^a
HD 251726	2360–237 ⁺²⁹⁵	0.9 ± 0.2	2.2 ^d	MWC 672	2942–218 ⁺²⁵⁵	0.3 ± 0.02	1.4 ^a
HD 25487	303–7 ⁺⁸	0.9 ± 0	0.6 ^a	MWC 677	2797–285 ⁺³⁵⁵	0.2 ± 0.01	2.3 ^a
HD 259431	711–23 ⁺²⁴	0 ± 0	1.3 ^a	MWC 678	3418–372 ⁺⁴⁶⁹	0 ± 0	1.6 ^a
V615 Cas	2445–214 ⁺²⁵⁸	2.8 ± ± 0	3.1 ^c	-	-	-	-

^aZhang et al. (2005); ^bStevens et al. (2017); ^cGontcharov (2012); ^dChen et al. (2016); ^eVarga et al. (2018); ^fSwihart et al. (2017)

Table 3. List of 35 of our program stars for which A_V values are adopted from the literature. Zhang et al. (2005) obtained A_V > 1.0 for 4 stars which are marked in bold here.

Name	A _V	Name	A _V
HD 10516	0.5 ³	HD 45542	0.1 ³
HD 109387	0.1 ⁴	HD 45725	0.2 ²
HD 12856	1.6 ³	HD 45726	0.2 ²
HD 144	0.3 ¹	HD 46131	0.03 ²
HD 20336	0.3 ⁴	HD 50658	0.2 ³
HD 20340	0.2 ³	HD 50820	2.1 ³
HD 23302	0.2 ⁴	HD 50868	0.2 ³
HD 23630	0.1 ¹	HD 51354	0.2 ³
HD 237091	2.8 ³	HD 53085	0.03 ³
HD 23862	0.2 ³	HD 53416	0.02 ³
HD 25940	0.5 ³	HD 5394	0.7 ³
HD 33328	0.1 ³	HD 58050	0.1 ³
HD 36012	0.3 ²	HD 58343	0.4 ⁴
HD 36376	0.6 ³	HD 60260	0.3 ³
HD 36576	0.6 ²	HD 62367	0 ⁴
HD 37115	0.1 ³	HD 89884	0.1 ⁴
HD 38010	0.8 ³	MWC 669	3.1 ³
HD 4180	0.3 ³	-	-

¹Swihart et al. (2017); ²Chen et al. (2016); ³Zhang et al. (2005); ⁴Gontcharov (2012)

Table 4. Estimated Balmer decrements, D_{34} and D_{54} for our program stars. Our measured equivalent widths (EW) of $H\alpha$, $H\beta$ and $H\gamma$ lines are listed in columns 2 to 4. EW_c in columns 5 to 7 denote the absorption corrected $H\alpha$, $H\beta$ and $H\gamma$ lines for the same stars. (-) sign in these columns denote emission, whereas positive value denotes absorption. Columns 8 and 9 present the estimated Balmer decrements i.e. $(D_{34})_c$ and $(D_{54})_c$ values, respectively with the associated errors for those 83 stars whose A_V values are estimated by us. The star, HD 60855 which shows $H\alpha$ in absorption after correcting for underlying stellar absorption, is marked in bold. For 5 other stars (marked with star), we could not confirm the spectral types from the literature. $H\beta$, $H\gamma$ lines are not visible in case of HD 45726 and HD 58343 (marked with asterisk) since Grism 7 spectra is not available for them.

Name	$H\alpha$ EW	$H\beta$ EW	$H\gamma$ EW	$H\alpha$ EW_c	$H\beta$ EW_c	$H\gamma$ EW_c	$(D_{34})_c$	$(D_{54})_c$
AS 1	-9.9	3.2	4.9	-16.4	-4.5	-3.5	1.5 \pm 0.2	1.1 \pm 0.1
AS 105	4	4.9	5.5	-1.6	-1.9	-1.9	0.3 \pm 0.03	1.5 \pm 0.2
AS 52	-31	0.8	4.3	-36.7	-6	-3.1	2.4 \pm 0.2	0.7 \pm 0.1
BD+102133*	-15.3	-0.6	-3.1	-	-	-	-	-
BD+55 81	3.1	4	5.2	-0.8	-0.4	0.8	0.6 \pm 0.1	-
BD+59 334	3.2	3.3	3.7	-0.8	-1	-0.7	0.2 \pm 0.02	1.7 \pm 0.2
BD+60 307	-13.9	1.23	3.2	-18.6	-4.3	-2.7	1.5 \pm 0.2	1.1 \pm 0.1
BD+60 368	2.9	2.9	5.2	-1.1	-1.4	0.7	0.2 \pm 0.02	-
BD+62 287	-10.4	5.5	8.2	-18.3	-4.1	-2	1.9 \pm 0.2	0.8 \pm 0.1
BD+62 292	0.9	2.4	3.3	-3.1	-1.9	-1.2	0.5 \pm 0.1	0.8 \pm 0.1
BD+62 300	-0.1	2.9	3.7	-4	-1.5	-0.7	1.7 \pm 0.2	1.6 \pm 0.2
CD-22 4761	-36.8	-3.1	-	-40.8	-7.4	-	3 \pm 0.4	-
HD 10516*	-28.6	-1.7	4.4	-	-	-	-	-
HD 109387	-18.8	3.2	5.7	-25.7	-5.2	-3.3	2.1	1.1
HD 12302	-33.7	-1.7	3	-37.6	-6.1	-1.4	3.1 \pm 0.5	1.6 \pm 0.2
HD 12856	-39.9	-3.1	1.3	-43.9	-7.4	-3.2	3.4	2.2
HD 12882	-24.8	-0.8	2.8	-29.5	-6.4	-3.1	1.8 \pm 0.2	0.7 \pm 0.1
HD 13051	-5.4	1.1	4.7	-9.3	-3.3	0.2	1 \pm 0.1	-
HD 13429	-0.8	5.4	5.9	-6.4	-1.4	-1.5	1.8 \pm 0.2	1.6 \pm 0.2
HD 144	-3.6	6.9	9.2	-15.8	-10.5	-8.9	1.2	1.7
HD 15238	-10.3	2.7	4.9	-16.6	-5	-3.5	1.8 \pm 0.2	1.5 \pm 0.2
HD 18552	-14.7	4.8	7.9	-22.2	-4.2	-1.9	2.4 \pm 0.3	0.9 \pm 0.1
HD 18877	5.4	8.4	9.8	-2.1	-0.6	0	1.4 \pm 0.1	-
HD 19243	-35.4	-2.9	-0.2	-39.2	-7.3	-4.7	1.8 \pm 0.2	1.2 \pm 0.1
HD 20017	-10.4	3.9	6.5	-16.8	-3.7	-1.9	1.8 \pm 0.2	0.7 \pm 0.1
HD 20134	2.9	5.3	6.2	-1.8	-0.3	0.4	1.8 \pm 0.2	-
HD 20336	-14.4	2	4.5	-19.1	-3.6	-1.4	1.9	0.9
HD 20340	4.8	5.9	6.8	-0.8	-0.9	-0.6	0.4	1
HD 21212	-54.4	-4.9	-	-59.1	-10.5	-	2 \pm 0.2	-
HD 21455	-0.5	7.2	8.5	-8	-1.9	-0.5	2.2 \pm 0.2	1.5 \pm 0.2
HD 21641	-8.1	9.6	11.8	-20.3	-7.8	-6.3	1 \pm 0.1	1 \pm 0.1
HD 218393	-21.3	-1.3	1.9	-26.9	-8.1	-5.5	1.3 \pm 0.1	1 \pm 0.1
HD 22780	4.7	7.8	9.1	-2.8	-1.2	-0.7	0.9 \pm 0.1	0.8 \pm 0.1
HD 232590	3.1	2.9	3.7	-0.8	-1.5	-0.8	0.2 \pm 0.02	0.7 \pm 0.1
HD 23302	-0.6	6.2	7.8	-7.5	-2.2	-1.2	1.4	0.9
HD 23552	-32.1	-3.2	-0.6	-40	-12.8	-10.8	1.3 \pm 0.1	1.2 \pm 0.1
HD 23630	-2.8	5.1	6	-10.3	-3.9	-3.8	1.3	1.6
HD 236935	-11.9	0.1	2.5	-15.8	-4.2	-1.9	1.6 \pm 0.2	1.2 \pm 0.1
HD 236940	-24.5	-1.7	2.5	-29.2	-7.3	-3.3	1.3 \pm 0.1	0.8 \pm 0.1
HD 237056	1.2	2.9	3.2	-2.8	-1.4	-1.3	0.7 \pm 0.1	1.8 \pm 0.2
HD 237060	-11.4	5.1	7.3	-23.7	-12.3	-10.8	0.8 \pm 0.1	1.1 \pm 0.1
HD 237091	2.8	3.9	3.7	-1.1	-0.5	-0.7	0.7	2.1
HD 237118	-13.3	4.8	7	-20.1	-3.6	-1.9	3 \pm 0.5	1.6 \pm 0.2
HD 237134	-38.2	-1.6	6.5	-46.1	-11.2	-3.7	2.2 \pm 0.2	1.1 \pm 0.1
HD 23862	-7.8	5.4	6.8	-15.7	-4.2	-3.5	1.7	1.4
HD 244894	-15.1	-1.2	-0.03	-18.9	-5.6	-4.4	2.7 \pm 0.4	2.9 \pm 0.3
HD 249695	-5.9	2.5	4.6	-9.8	-1.9	0.2	3 \pm 0.3	-
HD 251726	-41.3	2.9	-0.2	-45.2	-1.5	-4.6	9 \pm 0.9	4.6 \pm 0.5
HD 25487	6.9	11.6	11.8	-1	2	1.6	-	-
HD 25940	-25.8	2.23	5.7	-31.4	-4.6	-1.7	3.2	1
HD 259431	-61.9	-1.6	3.9	-68.7	-9.9	-5.1	2.8 \pm 0.3	0.8 \pm 0.1
HD 259597	-15.6	-0.6	2.4	-19.5	-4.9	-2.1	2.9 \pm 0.5	2.3 \pm 0.3
HD 259631	-32.9	-2.1	1.9	-36.8	-6.5	-2.5	4.2 \pm 0.4	2.4 \pm 0.3

Name	H α EW	H β EW	H γ EW	H α -EW_c	H β -EW_c	H γ -EW_c	(D ₃₄) _c	(D ₅₄) _c
HD 277707*	-29.2	-2.2	1.5	-	-	-	-	-
HD 2789	4.5	5.7	6.4	-1.1	-1.1	-0.4	0.4 \pm 0.04	1.4 \pm 0.1
HD 29441	-23.9	-1.6	3.3	-28.6	-7.2	-2.5	1.5 \pm 0.2	0.8 \pm 0.1
HD 29866	-11.8	4.6	6.3	-19.7	-4.9	-3.9	2 \pm 0.2	1.5 \pm 0.2
HD 33328	1.3	2.9	3.9	-3.4	-2.7	-1.9	0.4	1.1
HD 33357	3.3	4.5	5	-0.6	0.1	0.6	-	-
HD 33461	-8.9	-1.5	4.8	-13.6	-7.1	-1	0.6 \pm 0.1	0.2 \pm 0.02
HD 35345	-33.8	-3.2	-0.5	-37.6	-7.5	-4.9	2.6 \pm 0.3	2.1 \pm 0.2
HD 36012	-25.9	3.5	7.3	-30.7	-2.1	-0.1	6.1	0.3
HD 36376	-29.2	-1.9	3.7	-37.1	-11.4	-6.5	1.9	1.4
HD 36576	-32.3	-2.6	-0.2	-36.9	-8.2	-6	2	1.7
HD 37115	-26.3	4.4	7.4	-33.8	-4.7	-2.4	3	0.9
HD 37657	-20	-0.7	3.2	-25.7	-7.6	-4.2	1.4 \pm 0.1	0.8 \pm 0.1
HD 37806	-26.5	6.5	9.9	-38.7	-10.9	-8.1	1.4 \pm 0.1	1 \pm 0.1
HD 37967	-37.9	-2.1	5.5	-42.7	-7.7	-0.3	1.9 \pm 0.2	0.2
HD 38010	-36.8	-2.9	-0.4	-40.6	-7.3	-4.8	2.5	1.8
HD 38708	3.3	4.3	5.5	-2.3	-2.5	-1.9	0.4 \pm 0.04	1.1 \pm 0.1
HD 4180	-33.2	-1.8	3.8	-39.6	-9.5	-4.6	2	1
HD 45542	-2.8	5.8	6.8	-9.6	-2.6	-2.2	1.6	1.4
HD 45626	-3.6	4.2	4.9	-10	-3.5	-3.4	1.1 \pm 0.1	1.4 \pm 0.1
HD 45725	-32.8	-1.6	3.7	-38.8	-8.9	-4.2	1.9	0.9
HD 45726*	-30.3	-	-	-35	-	-	-	-
HD 45901	-22.6	-1.3	1.7	-27.3	-6.9	-4.1	1.2 \pm 0.1	0.9 \pm 0.1
HD 45910	-34	-5.4	1.4	-38.7	-11	-4.5	1.1 \pm 0.1	0.6 \pm 0.1
HD 46131	4.4	4.7	5.9	-1.6	-2.6	-2	0.2	1.2
HD 47359	-2.8	1.5	4.1	-6.8	-2.8	-0.3	1.8 \pm 0.2	1.3 \pm 0.1
HD 49330	-9.7	1.1	3.8	-14.4	-4.5	-2	3 \pm 0.4	2.7 \pm 0.4
HD 50658	4.2	6.1	7.7	-3.7	-3.5	-2.5	0.4	1
HD 50696	-9.7	1.1	3.8	-14.4	-4.5	-2	1.1 \pm 0.1	0.8 \pm 0.1
HD 50820	-10.5	-1.2	3.4	-16.1	-8	-4	2.9	2.8
HD 50868	-7.5	2.2	4.6	-12.2	-3.4	-1.2	1.3	0.7
HD 51193	-21.7	-1.5	2.7	-27.3	-8.3	-4.8	1 \pm 0.1	0.9 \pm 0.1
HD 51354	-17.7	2.2	5.1	-23.3	-4.7	-2.3	2.2	0.9
HD 51480*	-54.1	-6.3	-1.2	-	-	-	-	-
HD 53085	-17.7	2.2	5.1	-23.3	-4.7	-2.3	2	0.7
HD 53416	-5.2	7.5	8.5	-13.2	-2.1	-1.8	2.5	1.2
HD 5394	-31.7	-2.7	-0.4	-35.6	-7	-4.8	1.7	1.9
HD 55439	-5.6	3.7	5.4	-10.3	-1.9	-0.5	1.9 \pm 0.2	0.7 \pm 0.1
HD 55606	-57.9	-4.5	-0.1	-61.9	-8.8	-4.6	4.8 \pm 0.6	3.5 \pm 0.4
HD 55806	-10.7	2.3	6.4	-18.2	-6.7	-3.4	1.3 \pm 0.1	0.9 \pm 0.1
HD 58050	2.9	4.9	5.9	-1.8	-0.7	0.1	0.8	-
HD 58343*	-11.4	-	-	-16.1	-	-	-	-
HD 60260	-9.6	2.1	4.3	-15.2	-4.8	-3.2	1.6	1.2
HD 60855	9.6	15.1	14.9	4.9	9.5	9.1	-	-
HD 61205	11.8	15.8	17.4	-0.5	-1.6	-0.7	0.1 \pm 0.01	0.6 \pm 0.1
HD 61224*	-8.2	5.1	6.9	-	-	-	-	-
HD 62367	-9.2	6.1	8.5	-17.1	-3.5	-1.7	2	0.7
HD 65079	-17.5	1.4	4.5	-22.2	-4.2	-1.3	1.6 \pm 0.2	0.5 \pm 0.1
HD 698	-10.2	1.9	4.2	-17.7	-7.1	-5.6	1 \pm 0.1	1.1 \pm 0.1
HD 72043	-20.9	4.1	6.5	-27.4	-3.6	-1.8	3.4 \pm 0.3	1.1 \pm 0.1
HD 89884	-17.5	2.8	5.4	-23.9	-4.9	-3	2.1	1
HR 2142	-31.9	-2.2	2.4	-36.7	-7.8	-3.5	1.4 \pm 0.1	0.7 \pm 0.1
MWC 28	-40.5	-4	-0.6	-45.2	-9.6	-6.4	1.4 \pm 0.1	1 \pm 0.1
MWC 3	-37	-3.5	-0.8	-41	-7.8	-5.3	3.4 \pm 0.4	2.8 \pm 0.3
MWC 5	-14.8	-1.8	-0.3	-18.8	-6.1	-4.8	1.2 \pm 0.1	1.5 \pm 0.2
MWC 500	-7.1	2.9	4.2	-10.9	-1.4	-0.3	4.4 \pm 0.4	1.6 \pm 0.2
MWC 566	-68.7	-7.2	-1.6	-72.7	-11.4	-6.1	2.9 \pm 0.3	1.8 \pm 0.2
MWC 667	-19.7	-1.1	2.5	-24.4	-6.6	-3.4	1.3 \pm 0.1	1 \pm 0.1
MWC 669	-7.8	1.1	2.9	-11.7	-3.3	-1.6	1.5	0.9
MWC 672	-49.6	-4.4	0.4	-54.3	-9.9	-5.4	1.9 \pm 0.2	1.1 \pm 0.1
MWC 677	-34.1	-1.9	2.5	-38.8	-7.5	-3.3	1.8 \pm 0.2	0.9 \pm 0.1
MWC 678	-62.3	-4.8	-0.3	-67	-10.4	-6.2	1.9 \pm 0.2	0.9 \pm 0.1